

# Accepted Manuscript

Discovery of New Antimalarial Agents: Second-Generation Dual Inhibitors against FP-2 and PfDHFR via Fragments Assembly

Wenhua Chen, Zhenghui Huang, Wanyan Wang, Fei Mao, Longfei Guan, Yun Tang, Hualiang Jiang, Jian Li, Jin Huang, Lubin Jiang, Jin Zhu

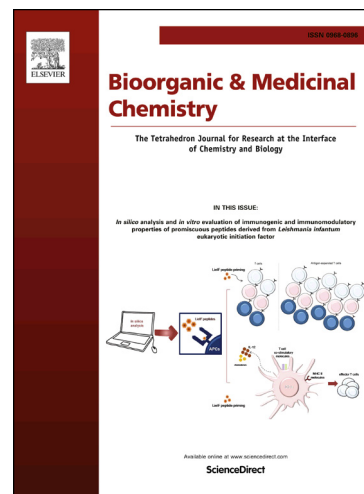
PII: S0968-0896(17)31607-3  
DOI: <https://doi.org/10.1016/j.bmc.2017.10.017>  
Reference: BMC 14022

To appear in: *Bioorganic & Medicinal Chemistry*

Received Date: 8 August 2017  
Revised Date: 7 October 2017  
Accepted Date: 16 October 2017

Please cite this article as: Chen, W., Huang, Z., Wang, W., Mao, F., Guan, L., Tang, Y., Jiang, H., Li, J., Huang, J., Jiang, L., Zhu, J., Discovery of New Antimalarial Agents: Second-Generation Dual Inhibitors against FP-2 and PfDHFR via Fragments Assembly, *Bioorganic & Medicinal Chemistry* (2017), doi: <https://doi.org/10.1016/j.bmc.2017.10.017>

This is a PDF file of an unedited manuscript that has been accepted for publication. As a service to our customers we are providing this early version of the manuscript. The manuscript will undergo copyediting, typesetting, and review of the resulting proof before it is published in its final form. Please note that during the production process errors may be discovered which could affect the content, and all legal disclaimers that apply to the journal pertain.



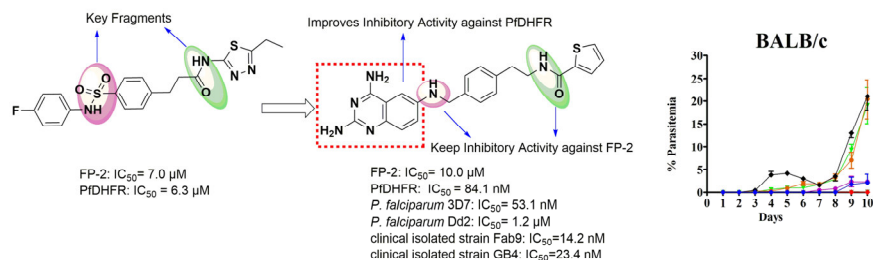
## Graphical Abstract

## Discovery of New Antimalarial Agents: Second-Generation Dual Inhibitors against FP-2 and PfDHFR via Fragments Assembly

Wenhua Chen<sup>a,†</sup>, Zhenghui Huang<sup>b,†</sup>, Wanyan Wang<sup>a,†</sup>, Fei Mao<sup>a</sup>, Longfei Guan<sup>a</sup>, Yun Tang<sup>a</sup>, Hualiang Jiang<sup>a</sup>, Jian Li<sup>a</sup>, Jin Huang<sup>a,\*</sup>, Lubin Jiang<sup>b,\*</sup>, Jin Zhu<sup>a,\*</sup>

<sup>a</sup> Shanghai Key Laboratory of New Drug Design, School of Pharmacy, East China University of Science and Technology, Shanghai 200237, China

<sup>b</sup> Key Laboratory of Molecular Virology & Immunology, Unit of Human Parasite Molecular and Cell Biology, Institute Pasteur of Shanghai, University of Chinese Academy of Science, 320 Yueyang Road, Shanghai 200031, China





## Discovery of New Antimalarial Agents: Second-Generation Dual Inhibitors against FP-2 and PfDHFR via Fragments Assembly

Wenhua Chen<sup>a,†</sup>, Zhenghui Huang<sup>b,†</sup>, Wanyan Wang<sup>a,†</sup>, Fei Mao<sup>a</sup>, Longfei Guan<sup>a</sup>, Yun Tang<sup>a</sup>, Hualiang Jiang<sup>a</sup>, Jian Li<sup>a</sup>, Jin Huang<sup>a,\*</sup>, Lubin Jiang<sup>b,\*</sup>, Jin Zhu<sup>a,\*</sup>

<sup>a</sup> Shanghai Key Laboratory of New Drug Design, School of Pharmacy, East China University of Science and Technology, Shanghai 200237, China

<sup>b</sup> Key Laboratory of Molecular Virology & Immunology, Unit of Human Parasite Molecular and Cell Biology, Institute Pasteur of Shanghai, University of Chinese Academy of Science, 320 Yueyang Road, Shanghai 200031, China

<sup>†</sup> These authors contributed equally to this work.

\* To whom correspondence should be addressed: [jinz@ecust.edu.cn](mailto:jinz@ecust.edu.cn), [huangjin@ecust.edu.cn](mailto:huangjin@ecust.edu.cn) or [lbjiang@ips.ac.cn](mailto:lbjiang@ips.ac.cn).

### ARTICLE INFO

### ABSTRACT

#### Article history:

Received

Received in revised form

Accepted

Available online

#### Keywords:

Antimalarial drug

*Plasmodium falciparum*

FP-2

PfDHFR

Dual inhibitor

Malaria parasites are a leading cause of worldwide mortality from infectious disease. Cysteine protease falcipain-2 (FP-2) and *Plasmodium falciparum* dihydrofolate reductase (PfDHFR) play vital roles, which are absolutely essential, in the parasite life cycle. In this study, based on the structures of uniform fragments of reported PfDHFR inhibitors and the first-generation dual inhibitors against FP-2 and PfDHFR, we identified a novel series of dual inhibitors through fragments assembly. Lead optimization led to the discovery of **24**, which showed high potency against FP-2 (IC<sub>50</sub>=10.0 μM), PfDHFR (IC<sub>50</sub>= 84.1 nM), *P. falciparum* 3D7 (IC<sub>50</sub>= 53.1 nM), clinical isolated strains Fab9 (IC<sub>50</sub>= 14.2 nM) and GB4 (IC<sub>50</sub>= 23.4 nM). The *in vivo* inhibition assays against *P. berghei* in 10 days indicated **24** had a more beneficial effect on the growth inhibition of *P. berghei* than artemisinin and an identical effect with pyrimethamine. Additionally, **24** moderately inhibited the proliferation of chloroquine-resistant *P. falciparum* Dd2 strain. Collectively, these data revealed that **24** could be an excellent lead compound as FP-2 and PfDHFR dual inhibitor for the treatment of malaria.

2017 Elsevier Ltd. All rights reserved.

### 1. Introduction

Malaria, a mosquito-borne disease caused by infection with *Plasmodium* parasites, is a devastating parasitic disease causing widespread mortality and morbidity across many parts of the developing world<sup>[1]</sup>. Nearly half the world's population are exposed in malaria endemic areas, and according to WHO 2016, malaria is responsible for an estimated 1.2 billion clinical cases of infection and 429,000 deaths in 2015 globally<sup>[2-3]</sup>. Children below five years of age and pregnant women living in poor countries are most vulnerable, it is considered that 303,000 malaria deaths happened in children aged under 5 years, which represented 70% of the global total deaths. Malaria remained a major killer of children, and it is estimated to take one child's life every 2 minutes<sup>[4-5]</sup>. Mammalian infection is initiated by the bite of *Plasmodium*-infected female *Anopheles* mosquitoes.<sup>[6-7]</sup> Among the species of plasmodia, *P. vivax* and *P. falciparum* are responsible for the majority of malaria infections and recrudescence infection via activation of dormant liver-stage hypozoites that re-establish the clinical blood-stage of infection.<sup>[8-12]</sup> Natural products and their derivatives, including artemisinin and its derivatives, are identified as first-line

antimalarial drugs used clinically. Although antimalarial drugs have successfully mitigated the epidemics in the past few decades, the control of malaria has been severely compromised in recent years, on account of the widespread resistance of *P. falciparum* to nearly all frontline therapeutics which were used for both prophylaxes and treatments<sup>[2,13-18]</sup>. Consequently, the requirement for the development and discovery of new antimalarial drugs, which are structurally distinct from existing drugs and endowed with novel mechanisms of action, is greatly exigent.<sup>[19-25]</sup>

In *P. falciparum*, various proteases catalyze the degradation of human hemoglobin, and the amino acids derived from this process are incorporated into parasite proteins or utilized for energy metabolism.<sup>[26]</sup> Cysteine protease falcipain-2 (FP-2) of *P. falciparum* is an indispensable protease involved in this metabolic process. FP-2, belonging to the family of cysteine proteases (papain-like enzymes known as clan CA), is expressed during the erythrocytic stage of the life cycle of the parasite.<sup>[27-28]</sup> In the past several years, various types of FP-2 inhibitors have been reported to be capable of inactivating the enzyme and a large number of studies have confirmed that inhibitors of FP-2 could block parasite hemoglobin hydrolysis, halt the

development of culture parasites, and these inhibitors are effective against murine malaria<sup>[29-39]</sup>. FP-2 has emerged as a promising target for the development of novel antimalarial drugs<sup>[40-43]</sup>

*P. falciparum* dihydrofolate reductase (PfDHFR) has received considerable attention for the prophylaxes and the treatments of *P. falciparum* infection.<sup>[44-45]</sup> The de novo synthesis of folate is required for DNA synthesis in *Plasmodium* species. The final step of folate synthesis is the enzymatic reduction of 7,8-dihydrofolate to 5,6,7,8-tetrahydrofolate, which is catalyzed by the enzyme PfDHFR.<sup>[46]</sup> Furthermore, PfDHFR is an essential metabolic enzyme that plays a critical role in one-carbon transfer reactions, including the biosynthetic pathways for deoxythymidine monophosphate (dTMP), purines, and several amino acids,<sup>[47]</sup> which is necessary for the synthesis of DNA. Consequently, a more powerful pesticidal effect could be achieved by inhibiting FP-2 and PfDHFR simultaneously. Such dual inhibitors might show a good synergetic effect, and overcome the drug-resistance and be capable of providing “a combination therapy” in a single agent<sup>[48]</sup>.

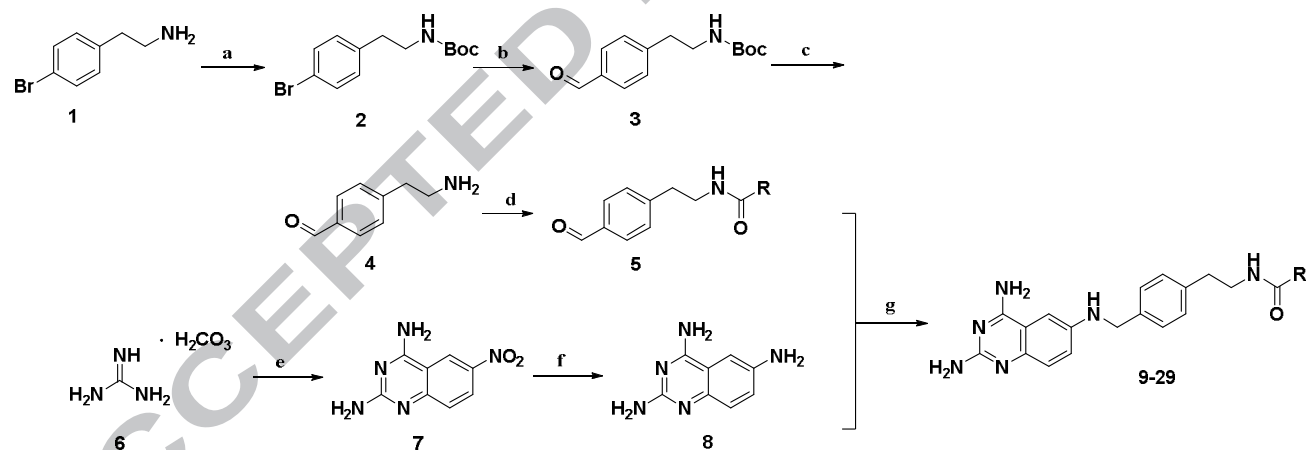
In this study, based on the structures of uniform fragments of reported PfDHFR inhibitors and the first-generation dual inhibitors against FP-2 and PfDHFR identified by us previously,<sup>[48]</sup> a novel series of second-generation dual inhibitors against FP-2 and PfDHFR had been designed through fragments assembly. In an attempt to gain novel structures with high potencies against both FP-2 and PfDHFR, we decided to explore the 2,4-diaminoquinazoline analogues (Structure **D**, Figure 2) on the basis of the computational analysis of three compounds (compounds **A-C**, Table 2), we exhaustively evaluated whether the type of substituent (R, Figure 2) at the terminal amide would

improve the pharmacological activity. Finally, a potent dual inhibitor (**24**) effectively inhibited the proliferation of *P. falciparum*, furthermore, the *in vivo* assays indicated **24** had a more beneficial effect on the growth inhibition of *P. berghei* than artemisinin. Thus, **24** was identified as a unique lead compound for the development of antimalarial drugs.

## 2. Results and discussion

### 2.1. Chemistry

As outlined in Scheme 1, *tert*-butyl(4-bromophenyl)-carbamate (**2**) was prepared from commercially available 2-(4-bromophenyl)ethan-1-amine (**1**) in the presence of (Boc)<sub>2</sub>O in CH<sub>2</sub>Cl<sub>2</sub> at 25 °C for 4 h in a yield of 84%. **2** was stirred with *n*-BuLi in THF at -78 °C under N<sub>2</sub> for 1 h, then DMF was added into the solution for another 1 h to give *tert*-butyl (4-formylphenyl)carbamate (**3**) in a yield of 70%. Further treatment of **3** with HCl-dioxane at 25 °C for 4 h gave 4-(2-aminoethyl)benzaldehyde (**4**) in a yield of 89%. Subsequent condensation of **4** with appropriate acids RCOOH in the presence of HOBt, EDCI and DIPEA in dichloromethane afforded amide **5** in good yields. 6-Nitroquinazoline-2,4-diamine (**7**) was prepared by reaction of guanidine carbonate (**6**) with 2-chloro-5-nitrobenzonitrile in DMF under reflux overnight in a yield of 60%. Reduction of **7** in the presence of 10% Pd/C and H<sub>2</sub> in MeOH and CH<sub>3</sub>COOH for 12 h in a yield of 80% provided quinazoline-2,4,6-triamine (**8**). Analogues **9-29** was performed by the reaction of **5** and **8**, via the condition using NaCNBH<sub>3</sub> in MeOH under reflux overnight in 30%-70% yields. All target compounds were confirmed to be ≥ 95% purity (Table S1, Supporting Information).



**Scheme 1.** Synthesis of target compounds **9-29**.

Reagents and conditions: (a) (Boc)<sub>2</sub>O, CH<sub>2</sub>Cl<sub>2</sub>, 25 °C, 4 h, 84%; (b) *n*-BuLi, THF, DMF, -78 °C, N<sub>2</sub>, 2 h, 70%; (c) HCl-dioxane, 25 °C, 4 h, 89%; (d) HOBt, EDCI, DIPEA, RCOOH, 25 °C, overnight; (e) 2-Chloro-5-nitrobenzonitrile, DMF, reflux, overnight, 60%; (f) 10% Pd/C, H<sub>2</sub>, MeOH, CH<sub>3</sub>COOH, 12 h, 80%; (g) NaCNBH<sub>3</sub>, MeOH, reflux, overnight, 30-70%.

### 2.2. Lead compound optimization and SAR

All synthesized analogues were evaluated for FP-2 enzymatic inhibitory activity with the cysteine protease inhibitor (**E-64**) as the reference and for PfDHFR enzymatic inhibitory activity with pyrimethamine as the reference. We assessed the inhibition rate (IR) of all the analogues against FP-2 and PfDHFR at 10 μM at first. Previously, we reported the first-generation dual inhibitors against FP-2 and PfDHFR based on

the compound **30**, which was randomly identified by screening FP-2 inhibitors in our laboratory, and gained compound **31** (**2o**) which exhibited a high enzymatic inhibition and a moderate *in vivo* antimalarial efficacy<sup>[48]</sup> (Figure 1). The SAR of the first-generation dual inhibitors showed that, (1) the best length of the middle phenyl linker was 2 methylene; (2) the sulfonamide and amide were important fragments, which formed hydrogen bonds with the surrounding amino acid residues, and (3) the best substituents were (hetero)aromatic rings<sup>[48]</sup> (Figure 1).

Considering the weak inhibitory activity against PfDHFR of the first-generation dual inhibitors, we firstly summarized the reported potent PfDHFR inhibitors (Table 1).

With analysis of SARs of the seven potent PfDHFR inhibitors<sup>[49-52]</sup>, the terminal heteroaromatic rings (2,4-diaminopteridine, 2,4-diaminoquinazoline, 2,4-diaminopyrimidine, 2,4-diaminotriazine), which were all 2,4-diamino heterocyclic fragments) were responsible for the inhibitory activities against PfDHFR and these 2,4-diamino heterocyclic fragments were the key pharmacophores. In an attempt to improve the inhibitory activity against PfDHFR, the three potent PfDHFR fragments were introduced into the left terminal substituent Ar. Considering the feasibility of the synthesis and novelty of scaffold, the sulfonamide was displaced with the secondary amine (green, Figure 1), and the amide position was interchanged (gray, Figure 1), therefore, three target compounds **A**, **B**, **C** were planned to synthesis (Figure 2).

Furthermore, the binding power was predicted by docking the three compounds (**A**, **B**, **C**) with proteins FP-2 and PfDHFR (PDB entry: 2OUL and 1J3I, respectively). In the docking process, standard-precision (SP) and extra-precision (XP) docking modes were respectively adopted to generate the minimized poses, the Glide scoring function (G-Score) was referred to select at most 10 poses for **A**, **B** and **C** upon visualized observation. As shown in Table 2, the lower predicted activity indicated the better inhibitory activity, thus comparing the predicted activity against FP-2 and PfDHFR, compound **B** was the best one, which demonstrated the enzymatic activity of the compound **B** might be the most potential one. Therefore, we decided to evaluate whether the type of substituent (R, Structure **D**, Figure 2) at the terminal amide would improve the pharmacological activity and explore the SAR of the 2,4-diaminoquinazoline analogues (**9-29**).

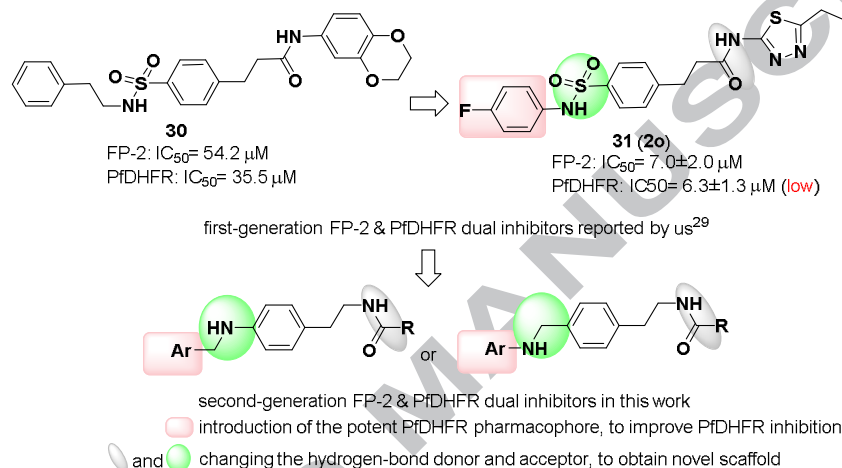


Figure 1. Chemical modification strategies for the second-generation dual inhibitors.

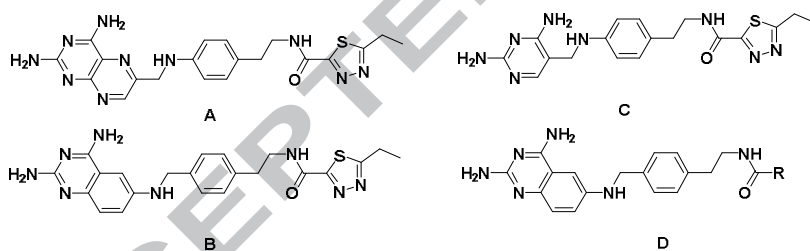
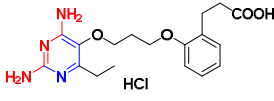
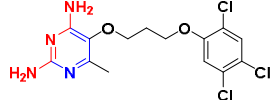
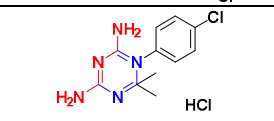
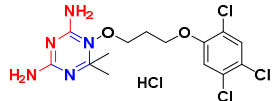


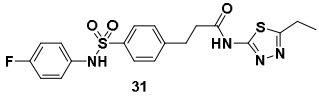
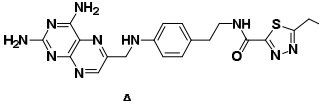
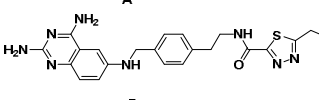
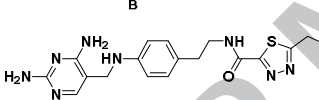
Figure 2. The target compounds A-C and structure D.

Table 1. Reported potent PfDHFR inhibitors.

Compd	Structure	PfDHFR IC <sub>50</sub> /nM	Pharmacophore
Methotrexate		84	
QN254		0.39	
Pyrimethamine		58	

P218		4.6	
P65		229	
Cycloguanil		1.5	
WR99210		0.57	

**Table 2.** Computational analysis of **31** and compounds (**A-C**).

Compound	Predicted activity kcal/mol <sup>a</sup>	
	FP-2	PfDHFR
	-5.01	-8.19
<b>A</b> 	-5.22	-9.59
<b>B</b> 	-7.14	-9.47
<b>C</b> 	-5.07	-8.10

<sup>a</sup>The crystal structures of falcipain-2 (FP-2) binding with cystatin and *P. falciparum* dihydrofolate reductase (PfDHFR) binding with WRA from *Plasmodium falciparum* were retrieved from the Protein Data Bank (PDB entry: 2OUL and 1J3I, respectively). Glide v5.5 (Schrodinger, Inc.) was used for molecular docking. The initial 3D structures of compound **A-C** were generated with the help of LigPrep v2.3 (Schrodinger, Inc.).

First, a small set of analogues with various electron-donating groups (EDGs) at the terminal phenyl ring (**9-15**, Table 3) were examined. Analogue **13** showed better IR against FP-2 at 10  $\mu$ M than **14** (IR = 52.6% vs 21.2%), moreover, **11**, which introduced an extra 3-methoxyl in **14**, slightly increased the IR against FP-2 (IR = 31.3% vs 21.2%). Interestingly, **12**, which replaced the 3-methoxyphenyl in **13** with 3,5-dimethoxyphenyl, decreased the inhibitory activity against FP-2 (IR = 41.1% vs 52.6%). Then we next brought in 1,4-benzodioxane (**9**) and 1,3-benzodioxole (**10**) at the terminal amide. Analogue **10** displayed the similar inhibitory activity against FP-2 as that of **31** (IR = 59.2% vs 64.7%), however analogue **9** showed poor inhibitory activity (IR = 34.9%). And analogues **9-14** demonstrated similar inhibitory activities against PfDHFR at 10  $\mu$ M (IR = 95.1%-100.0%), which were greater than **31** (IR = 59.2%).

To further develop this 2,4-diaminoquinazoline scaffold, we next explored analogues **16-21**, in which the electron-donating groups in the terminal phenyl were replaced by electron-withdrawing groups (EWGs) (Table 3). Analogues **16-18** with fluorophenyl showed the less inhibitory activities against FP-2 at 10  $\mu$ M (IR = 52.7%, 49.8%, 44.6% respectively) than **31** (IR = 64.7%) and the rank was 4-F > 3-F > 2-F. However, analogue **19** which introduced an additional 4-chloro in **18** improved significantly the inhibitory activity against FP-2 (IR =

62.4% vs 44.6%). Moreover, analogues **20-21** displayed obviously different inhibitory activities (IR = 21.5% vs 67.0%). Likewise, **16-18** and **20-21** showed potent inhibitory activities against PfDHFR at 10  $\mu$ M (IR = 94.7%-100.0%), by contrast **19** showed a poor inhibitory activity (IR = 68.2%).

With the intention of extending the R substitution scope at the terminal amide, the phenyl ring was replaced with other heteroaryl rings (**22-25**, Table 3). Adding a pyrid-4-yl group (**22**) and a furan-2-yl group (**23**) (IR = 22.9% and 28.9%) showed poor inhibitory activities against FP-2 obviously and **25** with 2-naphthalene represented a moderate inhibitory activity (IR = 46.4%). Nevertheless, **24** with a thiophene-2-yl dramatically enhanced the inhibitory activity against FP-2 (IR = 67.6%) compared to **22** and **23**. Additionally, **23-25** remained the potent inhibitory activities against PfDHFR (IR = 97.4%-100.0%) as well.

Then we further assessed the arylmethyl (**26**), arylethyl (**27**) and alkyl groups (**28-29**) in the terminal amide. **26-29** displayed the similar inhibitory activities against FP-2 as **31** (IR = 55.2%-66.6% vs 64.7%) and also remained potent inhibitory activities against PfDHFR (IR = 92.4%-99.9%). Analysis of the data shown in Table 3 revealed some noteworthy observations from the SAR study of analogues **9-29**: (1) the inhibitory

activities against FP-2 showed the phenyl substituents (R) with EDGs preferred 3-position (**11** vs **13** vs **14**) and the phenyl substituents with EWGs favored 4-position (**16** vs **17** vs **18**); (2) in the studied sets of the R substituents, the potency against FP-2

substantially increased in the order of (aryl)alkyl > EWG-aryl > EDG-aryl; and (3) in the test of inhibitory activities against PfDHFR, the R substituents could be well tolerated and eighteen analogues displayed high potencies (IR at 10  $\mu$ M > 90%).

**Table 3.** *In vitro* inhibitory activities against FP-2 and PfDHFR of analogues **9-29**

Compd	R	Inhibition @ 10 $\mu$ M		IC <sub>50</sub> $\pm$ SD <sup>a</sup>	
		FP-2 (%)	PfDHFR (%)	FP-2 / $\mu$ M	PfDHFR /nM
<b>31(2o)</b>	-	64.7	59.2	7.0 $\pm$ 2.0	6.3 $\pm$ 1.3 <sup>b</sup>
<b>E-64</b>	-	n.t. <sup>c</sup>	n.t. <sup>c</sup>	57.2 $\pm$ 8.2 <sup>d</sup>	n.t. <sup>c</sup>
<b>Pyrimethamine</b>	-	n.t. <sup>c</sup>	n.t. <sup>c</sup>	n.t. <sup>c</sup>	25.5 $\pm$ 6.7
<b>9</b>		34.9	100.0	n.t. <sup>c</sup>	80.9 $\pm$ 12.2
<b>10</b>		59.2	100.0	5.1 $\pm$ 2.6	26.2 $\pm$ 1.4
<b>11</b>		31.3	100.0	n.t. <sup>c</sup>	61.1 $\pm$ 3.0
<b>12</b>		41.1	100.0	n.t. <sup>c</sup>	32.1 $\pm$ 0.01
<b>13</b>		52.6	96.8	6.2 $\pm$ 1.0	39.6 $\pm$ 8.6
<b>14</b>		21.2	95.1	n.t. <sup>c</sup>	157.2 $\pm$ 12.7
<b>15</b>		37.6	51.2	n.t. <sup>c</sup>	n.t. <sup>c</sup>
<b>16</b>		52.7	96.7	6.7 $\pm$ 1.3	118.0 $\pm$ 6.0
<b>17</b>		49.8	98.5	n.t. <sup>c</sup>	50.6 $\pm$ 0.5
<b>18</b>		44.6	100.0	n.t. <sup>c</sup>	180.2 $\pm$ 13.9
<b>19</b>		62.4	68.2	9.1 $\pm$ 2.1	n.t. <sup>c</sup>
<b>20</b>		21.5	96.4	n.t. <sup>c</sup>	21.3 $\pm$ 0.1
<b>21</b>		67.0	94.7	10.0 $\pm$ 1.1	55.6 $\pm$ 13.7
<b>22</b>		22.9	51.5	n.t. <sup>c</sup>	n.t. <sup>c</sup>
<b>23</b>		28.9	97.8	n.t. <sup>c</sup>	107.4 $\pm$ 14.9
<b>24</b>		67.6	97.4	10.0 $\pm$ 0.3	84.1 $\pm$ 12.7

25		46.4	100.0	n.t. <sup>c</sup>	67.9±0.02
26		65.0	92.4	7.6±7.0	70.1±2.5
27		55.2	98.6	4.9±0.6	185.4±23.1
28		66.6	96.0	7.7±5.9	225.5±5.0
29		55.8	99.9	7.4±0.4	289.9±31.2

<sup>a</sup>Average of more than two experiments. <sup>b</sup>Unit:  $\mu\text{M}$ . <sup>c</sup>n.t. indicates no test. <sup>d</sup>Unit: nM.

### 2.3. Enzymatic Inhibition of Potent Analogues

Furthermore, ten analogues, i.e., **10**, **13**, **16**, **19**, **21**, **24** and **26-29**, were identified as inhibitors against FP-2 with IR > 50% at 10  $\mu\text{M}$  and eighteen analogues, i.e., **9-14**, **16-18**, **20-21**, **23-29**, were identified as potent inhibitors against PfDHFR with IR > 90% at 10  $\mu\text{M}$ . Therefore, they were further evaluated for half maximal inhibitory concentration ( $\text{IC}_{50}$ ) of two targets, respectively. As shown in Table 3, the ten inhibitors against FP-2 demonstrated similar enzymatic inhibitory activities ( $\text{IC}_{50}$  = 4.9-10.0  $\mu\text{M}$ ), **10** and **27** displayed slightly better than that of **31** ( $\text{IC}_{50}$  = 5.1  $\mu\text{M}$ , 4.9  $\mu\text{M}$  vs 7.0  $\mu\text{M}$ ). The eighteen potent inhibitors against PfDHFR presented more potent than **31** ( $\text{IC}_{50}$  = 21.3-289.9 nM vs 6.3  $\mu\text{M}$ ). Analogue **12** performed a better inhibitory activity against PfDHFR than **11**, **13** and **14** ( $\text{IC}_{50}$  = 32.1 nM vs 61.1 nM, 39.6 nM and 157.2 nM respectively), which indicated the EDGs disfavored 4-position substituents. And **17**, **20** and **21** with EWGs displayed more potent activities against PfDHFR than **16** and **18** ( $\text{IC}_{50}$  = 21.3-55.6 nM vs 118.0-180.2 nM). Analogues **23-29** showed slightly less inhibitory activities against PfDHFR than **9-14**, which were substituted with EDGs ( $\text{IC}_{50}$  = 67.9-289.9 nM vs 26.2-157.2 nM). In the examination of the R substituents elicited the potency against

PfDHFR substantially increased in the order of EDG-aryl > EWG-aryl > (aryl)alkyl.

### 2.4. In Vitro Inhibitory Against Multi-Drug-Sensitive *P. falciparum* 3D7

From the results described above, six analogues, including **10**, **13**, **16**, **21**, **24** and **26** were identified as potent dual inhibitors against both FP-2 and PfDHFR ( $\text{IC}_{50}$  = 5.1-10.0  $\mu\text{M}$  against FP-2,  $\text{IC}_{50}$  = 26.2-118.0 nM against PfDHFR). Therefore, these six analogues were next evaluated in the inhibitory activity against the blood stage of the multi-drug-sensitive *P. falciparum* 3D7 strain. As shown in Figure 3, the selected analogues together with artemisinin (Art) and compound **31** were tested in 3D7 cells. All the six analogues performed nanomolar potencies against 3D7 parasites ( $\text{IC}_{50}$  = 53.1-390.9 nM), while **31** displayed poor potency against 3D7 parasites (Inhibition Rate [IR] = 7.9% @ 20  $\mu\text{M}$ ), demonstrating that the structural modification strategy employed in this study is efficient and valuable for improvement of the antimalarial potency. Moreover, **13** and **24** showed the most potent activities against the parasites ( $\text{IC}_{50}$  = 53.1 nM and 60.5 nM), thus the two analogues were selected for further development.

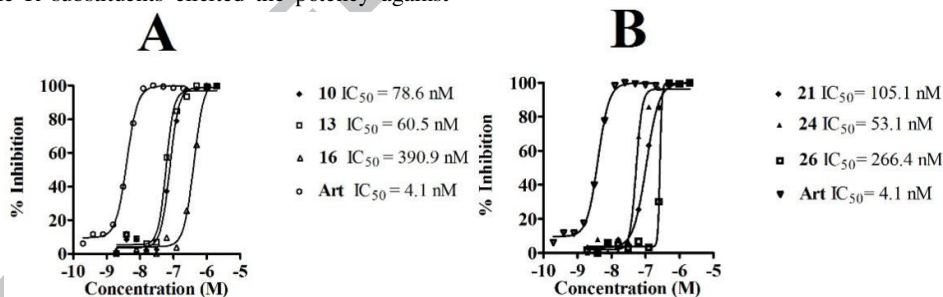


**Figure 3.** *In vitro* inhibitory activities against multi-drug-sensitive *P. falciparum* (3D7). (A) The inhibitory activities of analogues **10**, **13**, **16** and Art against *P. falciparum* (3D7); (B) the inhibitory activities of analogues **21**, **24**, **26** and Art against *P. falciparum* (3D7).

### 2.5. In Vivo Antimalarial Efficacy

To assess the *in vivo* antimalarial efficacies of **13** and **24**, the BALB/c mouse infected with the rodent parasite *P. berghei* were orally dosed daily with **13** and **24** for 4 days (Figure 4) and we used Art and pyrimethamine as the reference. **24** had a

significant inhibition in parasitaemia of 20 mg/kg (body weight) after the oral dose, moreover, **24** at 20 mg/kg demonstrated similar antimalarial efficacy as that of pyrimethamine, which were more effective than Art at 20 mg/kg. Meanwhile, **13** at 20 mg/kg dose also significantly inhibited the growth, although less effective than Art at 20 mg/kg.

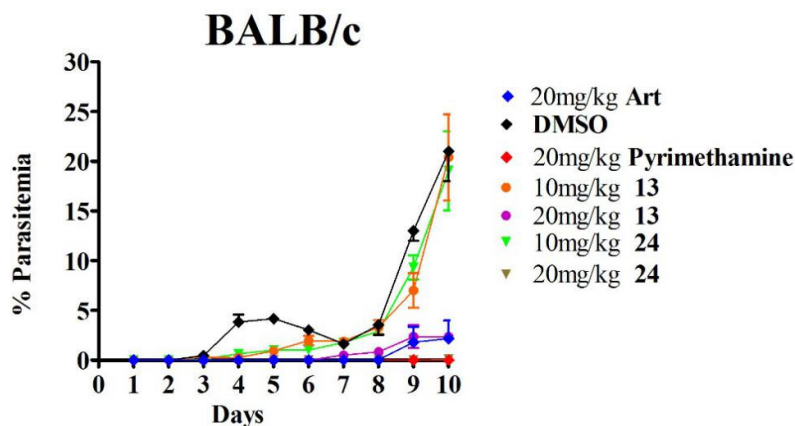


**Figure 4.** *In vivo* antimalarial efficacies against rodent parasite *Plasmodium berghei* in the BALB/c mouse model.

### 2.6. *In vitro* inhibitory against chloroquine-resistant *P. falciparum* Dd2 and clinical isolated strains

The remarkable antimalarial efficacies of analogues **13** and **24** supported that the two compounds were potent antimalarial agents, especially for **24**. To further evaluate the antimalarial potential of **13** and **24**, we tested the two compounds against *P. falciparum* Dd2 strain which carry a phenotype of resistance to chloroquine<sup>[26, 53]</sup>. As shown in Figure 5A, **13** and **24** displayed micromolar potency against Dd2 ( $IC_{50} = 2.2 \mu M$  and  $1.2 \mu M$ ), while pyrimethamine presented less effective

inhibition against Dd2 ( $IC_{50} > 10 \mu M$ ) and compound **31** displayed similar poor potency against Dd2 ( $IR = 6.2\% @ 20 \mu M$ ), which indicated analogues **13** and **24** could also inhibit the growth of resistant *P. falciparum*. Furthermore, we next evaluated the inhibitory activities of compound **24** against two clinical isolated strains, Fab9 and GB4. To our delight, as shown in Figure 5B, **24** displayed potent inhibitory activities against the two clinical isolated strains ( $IC_{50} = 14.2 nM$  against Fab9 and  $IC_{50} = 23.4 nM$  against GB4). These results indicated **24** could be a promising antimalarial lead compound.

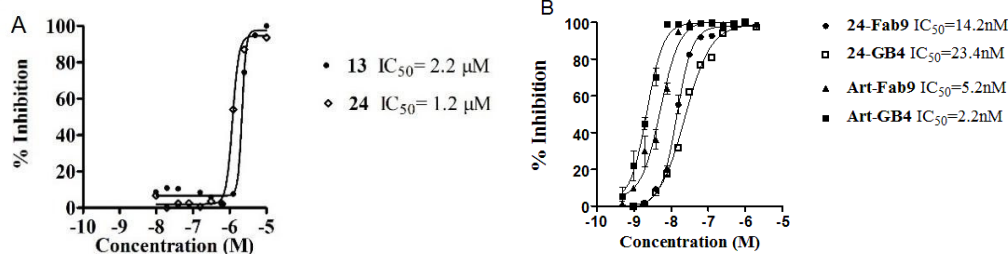
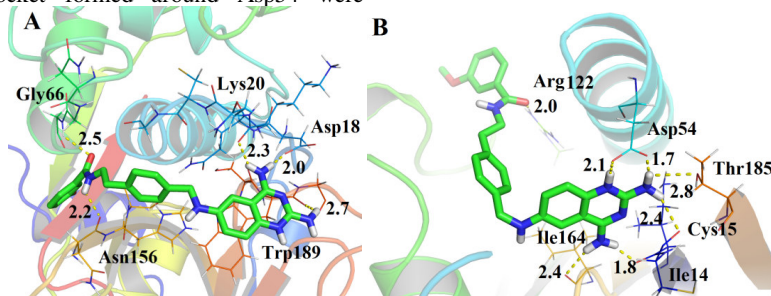


**Figure 5.** Inhibitory activities against chloroquine-resistant *P. falciparum* (Dd2) and two clinical isolated strains. (A) *In vitro* inhibitory activities of analogues **13** and **24** against chloroquine-resistant *P. falciparum* (Dd2); (B) *In vitro* inhibitory activities of analogue **24** and Art against two clinical isolated strains, Fab9 and GB4.

### 2.7. Molecular Docking Studies

To understand the structural basis for the inhibitory activities of the inhibitors against FP-2 and PfDHFR, the 3D binding models of analogues **13** and **24** with FP-2 and PfDHFR were studied by molecular docking (Figure 6). Figures 6A and 6C showed the predicted binding poses of **13** and **24** in the catalytic site of FP-2, respectively. The amide moieties of **13** and **24** directly interacted with Asn156 and Gly66 via H-bonds, meanwhile, the terminal 2,4-diaminoquinazoline group interacted with Asp18 and Lys20 via H-bonds, and **13** formed an additional H-bond with Trp189. For PfDHFR (Figures 6B and 6D), the catalytic subpocket formed around Asp54 were

occupied by the 2,4-diaminoquinazoline group in both **13** and **24**. The 2,4-diaminoquinazoline groups formed a complicated hydrogen-bond network with Asp54, Ile14, Cys15 and Ile164, respectively, which contributed significantly to the higher affinity of **13** and **24**. In the both cases of PfDHFR, the amide groups formed H-bonds with the key residue Arg122. The binding modes indicated the 2,4-diaminoquinazoline group was the critical fragment effecting the inhibitory activity against PfDHFR, meanwhile, the improved PfDHFR inhibitory activities of the twenty-one analogues also exhibited 2,4-diaminoquinazoline group was the critical pharmacophore for the PfDHFR inhibition.



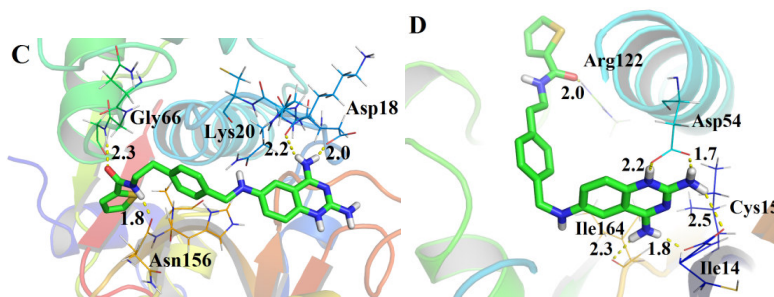


**Figure 6.** Molecular docking studies on **13** and **24**. Docked poses of **13** (green sticks) (A), and **24** (green sticks) (C) in the active sites of FP-2. Docked poses of **13** (green sticks) (B), and **24** (green sticks) (D) in the active sites of PfDHFR. Key residues of the binding pocket are shown as lines. Hydrogen bonds are shown with yellow dash lines.

### 3. Conclusion

In summary, we have identified a novel series of 2,4-diaminoquinazoline analogues (**9-29**) derived from **31** (**2o**) as FP-2 and PfDHFR dual inhibitors. On the basis of the structure of the lead compound **31**, twenty-one completely novel 2,4-diaminoquinazoline analogues have been synthesized and tested in FP-2 and PfDHFR enzymatic inhibitory activities. Ten analogues, i.e., **10**, **13**, **16**, **19**, **21**, **24** and **26-29**, showed good inhibitory activities against FP-2 ( $IC_{50}$  = 4.9-10.0  $\mu$ M) and eighteen analogues, i.e., **9-14**, **16-18**, **20-21**, **23-29**, displayed potent potencies against PfDHFR ( $IC_{50}$  = 21.3-289.9 nM). The most potent analogue (**20**) demonstrated a PfDHFR inhibitory capability that was about 295 times higher than **31**. Preliminary SARs were obtained, which showed that the amide and secondary amine groups of new analogues inherited FP-2 inhibitory activity from **31** and 2,4-diaminoquinazoline groups contributed to the dramatic enhancement of the inhibitory activity against PfDHFR. The molecular docking results also validated that the 2,4-diaminoquinazoline ring formed a complicated hydrogen-bond network with Asp54, Ile14, Cys15 and Ile164 in the catalytic subpocket of the PfDHFR enzyme. Additionally, in the studied sets of the R substituents, the potency against FP-2 substantially increased in the order of (aryl)alkyl > EWG-aryl > EDG-aryl, however, the potency against PfDHFR increased in the order of EDG-aryl > EWG-aryl > (aryl)alkyl. The *in vitro* inhibitory activity against *P. falciparum* with multi-drug-sensitive strain 3D7 further confirmed that the two analogues (**13** and **24**) were the most potent inhibitors against parasites ( $IC_{50}$  = 53.1 nM and 60.5 nM). In the BALB/c mouse model, **24** (20 mg/kg) had a similar antimalarial efficacy as pyrimethamine (20 mg/kg), which were more effective than Art (20 mg/kg). Meanwhile, **13** (20 mg/kg) dose also significantly inhibited the growth, although less effective than Art (20 mg/kg). To our delight, **13** and **24** inhibited chloroquine-resistant *P. falciparum* strain Dd2 ( $IC_{50}$  = 2.2  $\mu$ M and 1.2  $\mu$ M) which were superior to pyrimethamine ( $IC_{50}$  > 10  $\mu$ M), and **24** also displayed potent inhibitory activities against clinical isolated strains Fab9 and GB4 ( $IC_{50}$  = 14.2 nM and 23.4 nM respectively). Overall, **24** has the potential as a good antimalarial lead compound with novel mechanisms of action.

### 4. Experimental

#### 4.1. Synthesis General

Reagents and solvents were purchased from Adamas-Beta, J & K, Energy Chemical, Target Molecule, TCI, Alfa Aesar, and Acros, and were used without further purification. Analytical thin-layer chromatography (TLC) was conducted on HSGF 254 plates (150–200  $\mu$ m thickness; Yantai Huiyou Co., China) and spots were visualized with UV light. Yields were not optimized.

Melting points were measured in capillary tubes on an SGW X-4 melting point apparatus without correction. Nuclear magnetic resonance (NMR) spectroscopy was performed on a Bruker AMX-400 NMR (TMS as internal standard). Chemical shifts were reported in parts per million (ppm,  $\delta$ ) relative to tetramethylsilane. Proton coupling patterns were described as singlet (s), doublet (d), triplet (t), quartet (q), multiplet (m), and doublet of doublets (dd). High-resolution mass spectra (HRMS) were obtained on a Waters GCT Premie or Waters LCT using electron ionization (EI). HPLC analysis of analogues **9-29** was performed on an Agilent 1100 system equipped with a quaternary pump and a diode-array detector (DAD). The peak purity was verified by UV spectroscopy. All analogues were confirmed to be  $\geq 95\%$  purity.

#### 4.2. Synthesis of tert-butyl (4-bromophenethyl)carbamate (**2**)

To a suspension of 2-(4-bromophenyl)ethan-1-amine (**1**) (3.1 mL, 20 mmol) in  $CH_2Cl_2$  (30 mL) was added dropwise (Boc)<sub>2</sub>O (5.97 mL, 26 mmol) at 25 °C and the solution was stirred for 4 h. After the reaction completed, the solvent was removed under reduced pressure. The residue was dissolved in water, then the aqueous solution was extracted with ethyl acetate (50 mL  $\times$  3). The combined organic layers were washed with brine, dried over anhydrous sodium sulfate, and concentrated to give the crude product, which was purified by column chromatography to give *tert*-butyl(4-bromophenethyl)-carbamate (**2**) (5.0 g, 84% yield) as a white solid. <sup>1</sup>H NMR (400 MHz,  $CDCl_3$ )  $\delta$ : 7.42 (d,  $J$  = 8.2 Hz, 2H), 7.07 (d,  $J$  = 8.1 Hz, 2H), 4.52 (s, 1H), 3.35 (s, 2H), 2.75 (t,  $J$  = 6.9 Hz, 2H), 1.43 (s, 9H).

#### 4.3. Synthesis of tert-butyl (4-formylphenethyl)carbamate (**3**)

To a suspension of *tert*-butyl(4-bromophenethyl)-carbamate (**2**) (1.50 g, 5 mmol) in THF (35 mL) was cooled to -78 °C under  $N_2$ . Then *n*-BuLi (4.58 mL, 11 mmol, 2.4 M in THF) was added dropwise at -78 °C and after the mixture was stirred for 1 h, DMF (0.96 g, 12.5 mmol) was added dropwise at -78 °C and the mixture was stirred for another 1 hour. After the reaction completed, the solvent was removed under reduced pressure. The residue was dissolved in water, then the aqueous solution was extracted with ethyl acetate (50 mL  $\times$  3). The combined organic layers were washed with brine, dried over anhydrous sodium sulfate, and concentrated to give the crude product, which was purified by column chromatography to give *tert*-butyl(4-formylphenethyl)-carbamate (**3**) (0.87 g, 70% yield) as a yellow liquid. <sup>1</sup>H NMR (400 MHz,  $CDCl_3$ )  $\delta$ : 9.99 (s, 1H), 7.83 (d,  $J$  = 7.9 Hz, 2H), 7.37 (d,  $J$  = 7.9 Hz, 2H), 4.58 (s, 1H), 3.39 (m, 2H), 2.89 (t,  $J$  = 7.0 Hz, 2H), 1.43 (s, 9H).

#### 4.4. Synthesis of 4-(2-aminoethyl)benzaldehyde (**4**)

To a suspension of *tert*-butyl(4-formylphenethyl)-

carbamate (**3**) (0.75 g, 3 mmol) in dioxane (10 mL) was added HCl-dioxane (1.5 mL, 6 mmol, 4 M in dioxane) in dropwise. Then the mixture was stirred at 25 °C for 4 h. The solvent was removed under reduced pressure and the residue was dissolved in water, the aqueous solution was extracted with ethyl acetate (50 mL × 3). The combined organic layers were washed with brine, dried over anhydrous sodium sulfate and concentrated to give the crude product, which was purified by column chromatography to give 4-(2-aminoethyl)-benzaldehyde (**4**) (0.40 g, 89% yield) as a yellow liquid. <sup>1</sup>H NMR (400 MHz, CDCl<sub>3</sub>) δ: 9.96 (s, 1H), 8.04–7.96 (m, 2H).

#### 4.5. Synthesis of 6-nitroquinazoline-2,4-diamine (**7**)

To a suspension of guanidine carbonate (**6**) (1.21 g, 10 mmol) and 2-chloro-5-nitrobenzonitrile (1.83 g, 10 mmol) in DMF (50 mL) was stirred under reflux overnight. Then the mixture was cooled to room temperature and the mixture was dissolved in water, then the aqueous solution was extracted with ethyl acetate (50 mL × 3). The combined organic layers were washed with brine, dried over anhydrous sodium sulfate and concentrated to give the crude product, which was purified by column chromatography to give 6-nitroquinazoline-2,4-diamine (**7**) (1.23 g, 60% yield) as a red solid. <sup>1</sup>H NMR (400 MHz, DMSO-*d*<sub>6</sub>) δ: 9.08 (d, *J* = 2.4 Hz, 1H), 8.22 (dd, *J* = 9.3, 2.4 Hz, 1H), 8.11–7.55 (m, 2H), 7.22 (d, *J* = 9.3 Hz, 1H), 6.95–6.56 (m, 2H).

#### 4.6. Synthesis of quinazoline-2,4,6-triamine (**8**)

To a suspension of 6-nitroquinazoline-2,4-diamine (**7**) (1.03 g, 5 mmol) in MeOH (20 mL) and CH<sub>3</sub>COOH (1 mL) was added 10% Pd/C (0.21 g) under H<sub>2</sub>, and the mixture was at 50 °C stirred for 12 h. Then the reaction mixture was filtered, the filtrate was removed under reduced pressure and the residue was dissolved in water, then the aqueous solution was extracted with ethyl acetate (50 mL × 3). The combined organic layers were washed with brine, dried over anhydrous sodium sulfate and concentrated to give the crude product, which was purified by column chromatography to give quinazoline-2,4,6-triamine (**8**) (0.70 g, 80% yield) as a yellow solid. <sup>1</sup>H NMR (400 MHz, DMSO-*d*<sub>6</sub>) δ: 7.78 (s, 2H), 7.43 (s, 2H), 7.10 (d, *J* = 8.9 Hz, 2H), 7.07–7.02 (m, 1H), 5.24 (s, 2H).

#### 4.7. General procedure for Synthesis of *N*-(4-formylphenethyl)-amide (**5**) and *N*-(4-(((2,4-diaminoquinazolin-6-yl)amino)methyl)phenethyl)amide (**9-29**)

To a solution of corresponding acids (RCOOH, 0.63 mmol), HOBt (170 mg, 1.26 mmol), EDCI (242 mg, 1.26 mmol), and DIPEA (0.208 mL, 1.26 mmol) were added to DMA (60 mL), and then **4** (186 mg, 1.26 mmol) were added, the mixture was stirred overnight. The mixture was dissolved in water, then the aqueous solution was extracted with ethyl acetate (50 mL × 3). The combined organic layers were washed with brine, dried over anhydrous sodium sulfate and concentrated to give the crude product, which was purified by column chromatography to give *N*-(4-formylphenethyl)amide (**5**) in a good yield. Then the mixture of **5** and **7** was added NaCNBH<sub>3</sub> in MeOH and the solution was stirred under reflux overnight. After reaction completed, the solvent was removed under reduced pressure and the residue was dissolved in water, the aqueous solution was extracted with ethyl acetate (50 mL × 3). The combined organic layers were washed with brine, dried over anhydrous sodium sulfate and concentrated to give the crude product, which was purified by column chromatography to afford the corresponding compounds (**9-29**) in good yields.

#### 4.7.1. *N*-(4-(((2,4-diaminoquinazolin-6-yl)amino)methyl)phenethyl)-2,3-dihydrobenzo[*b*]-[1,4]dioxine-6-carboxamide (**9**)

Green solid, 32% yield. mp: 118–120 °C; <sup>1</sup>H NMR (400 MHz, DMSO-*d*<sub>6</sub>) δ: 8.75 (d, *J* = 11.0 Hz, 1H), 8.55 (s, 1H), 8.46 (t, *J* = 5.2 Hz, 1H), 7.99–7.82 (m, 1H), 7.60–7.31 (m, 6H), 7.30–7.11 (m, 4H), 6.92 (dd, *J* = 14.4, 7.7 Hz, 1H), 6.54 (t, *J* = 5.8 Hz, 1H), 4.16 (s, 2H), 3.64–3.55 (m, 2H), 3.20–3.06 (m, 4H), 2.80 (t, *J* = 7.4 Hz, 2H). <sup>13</sup>C NMR (100 MHz, DMSO-*d*<sub>6</sub>) δ: 165.79, 163.01, 153.68, 146.42, 146.34, 143.30, 138.58, 137.59, 130.71, 129.01, 128.18, 127.99, 124.58, 121.04, 117.16, 116.62, 110.50, 102.06, 64.77, 64.44, 42.03, 41.33, 35.22. HRMS(EI) *m/z* calcd for C<sub>26</sub>H<sub>26</sub>N<sub>6</sub>O<sub>3</sub>(M<sup>+</sup>) 470.2066, found 470.2064.

#### 4.7.2. *N*-(4-(((2,4-diaminoquinazolin-6-yl)amino)methyl)phenethyl)benzo[*d*][1,3]dioxole-5-carboxamide (**10**)

Green solid, 35% yield. mp: 288–290 °C; <sup>1</sup>H NMR (400 MHz, DMSO-*d*<sub>6</sub>) δ: 8.85 (t, *J* = 6.0 Hz, 1H), 8.70–8.41 (m, 3H), 8.09–7.90 (m, 2H), 7.60 (ddd, *J* = 6.8, 4.8, 1.7 Hz, 1H), 7.34 (d, *J* = 8.0 Hz, 4H), 7.21 (dd, *J* = 7.3, 3.3 Hz, 5H), 6.51 (t, *J* = 5.9 Hz, 1H), 4.28 (d, *J* = 5.7 Hz, 2H), 3.52 (dd, *J* = 14.5, 6.5 Hz, 2H), 3.17 (d, *J* = 4.8 Hz, 1H), 2.84 (t, *J* = 7.5 Hz, 2H). <sup>13</sup>C NMR (100 MHz, DMSO-*d*<sub>6</sub>) δ: 165.70, 162.68, 155.35, 150.03, 147.73, 145.38, 138.53, 137.79, 129.02, 128.19, 124.37, 122.50, 120.54, 110.72, 108.29, 107.66, 102.09, 101.47, 46.89, 41.42, 35.26. HRMS(EI) *m/z* calcd for C<sub>25</sub>H<sub>24</sub>N<sub>6</sub>O<sub>3</sub>(M<sup>+</sup>) 456.1910, found 456.1911.

#### 4.7.3. *N*-(4-(((2,4-diaminoquinazolin-6-yl)amino)methyl)phenethyl)-3,4-dimethoxybenzamide (**11**)

Green solid, 42% yield. mp: 289–291 °C; <sup>1</sup>H NMR (400 MHz, DMSO-*d*<sub>6</sub>) δ: 8.50 (t, *J* = 5.4 Hz, 1H), 7.89 (d, *J* = 8.4 Hz, 1H), 7.64 (d, *J* = 8.3 Hz, 1H), 7.41 (ddd, *J* = 36.7, 19.6, 5.0 Hz, 7H), 7.22 (d, *J* = 7.7 Hz, 4H), 7.00 (d, *J* = 8.4 Hz, 1H), 6.53 (t, *J* = 5.9 Hz, 1H), 4.29 (d, *J* = 5.8 Hz, 2H), 3.80 (t, *J* = 6.4 Hz, 6H), 3.44 (dd, *J* = 14.3, 6.1 Hz, 2H), 2.87–2.76 (m, 2H). <sup>13</sup>C NMR (100 MHz, DMSO-*d*<sub>6</sub>) δ: 165.75, 162.75, 154.60, 147.50, 146.75, 144.43, 138.72, 137.80, 129.89, 128.30, 127.56, 124.40, 120.79, 116.92, 110.66, 108.59, 102.16, 60.22, 59.88, 44.10, 41.60, 35.20. HRMS(EI) *m/z* calcd for C<sub>26</sub>H<sub>28</sub>N<sub>6</sub>O<sub>3</sub>(M<sup>+</sup>) 427.2223, found 427.2222.

#### 4.7.4. *N*-(4-(((2,4-diaminoquinazolin-6-yl)amino)methyl)phenethyl)-3,5-dimethoxybenzamide (**12**)

Green solid, 45% yield. mp: 222–224 °C; <sup>1</sup>H NMR (400 MHz, DMSO-*d*<sub>6</sub>) δ: 8.53 (s, 1H), 7.36 (d, *J* = 7.6 Hz, 2H), 7.20 (d, *J* = 8.4 Hz, 2H), 7.09–6.83 (m, 7H), 6.63 (s, 1H), 5.86 (s, 1H), 5.43 (s, 2H), 4.24 (s, 2H), 3.77 (s, 4H), 3.43 (s, 2H), 2.81 (s, 2H). <sup>13</sup>C NMR (100 MHz, DMSO-*d*<sub>6</sub>) δ: 166.14, 162.47, 160.75, 158.11, 144.21, 138.36, 137.15, 129.44, 129.15, 128.97, 128.26, 124.78, 121.89, 113.05, 110.65, 105.53, 55.86, 47.16, 41.44, 35.21. HRMS(EI) *m/z* calcd for C<sub>26</sub>H<sub>28</sub>N<sub>6</sub>O<sub>3</sub>(M<sup>+</sup>) 427.2223, found 427.2220.

#### 4.7.5. *N*-(4-(((2,4-diaminoquinazolin-6-yl)amino)methyl)phenethyl)-3-methoxybenzamide (**13**)

Green solid, 55% yield. mp: 150–152 °C; <sup>1</sup>H NMR (400 MHz, DMSO-*d*<sub>6</sub>) δ: 8.55 (t, *J* = 5.5 Hz, 1H), 8.35 (s, 2H), 7.45–7.29 (m, 5H), 7.28–6.98 (m, 8H), 6.42 (s, 1H), 4.26 (d, *J* = 6.0 Hz, 2H), 3.77 (s, 3H), 3.44 (dd, *J* = 14.0, 6.1 Hz, 2H), 2.80 (t, *J* = 7.5 Hz, 2H). <sup>13</sup>C NMR (100 MHz, DMSO-*d*<sub>6</sub>) δ: 166.34, 162.05, 159.59, 158.06, 143.74, 138.38, 138.25, 136.50, 129.87, 128.98, 128.26, 124.44, 124.00, 119.79, 117.33, 112.81, 111.11, 101.00, 55.69, 47.18, 41.42, 35.24. HRMS(EI) *m/z* calcd for C<sub>25</sub>H<sub>26</sub>N<sub>6</sub>O<sub>2</sub>(M<sup>+</sup>) 422.2117, found 422.2115.

4.7.6. *N*-(4-(((2,4-diaminoquinazolin-6-yl)amino)methyl)phenethyl)-4-methoxybenzamide (**14**)

Green solid, 50% yield. mp: 279–281 °C; <sup>1</sup>H NMR (400 MHz, DMSO-*d*<sub>6</sub>) δ: 8.40 (dd, *J* = 16.8, 11.4 Hz, 3H), 7.77 (d, *J* = 8.7 Hz, 2H), 7.30 (d, *J* = 7.8 Hz, 2H), 7.16 (t, *J* = 7.4 Hz, 7H), 6.94 (d, *J* = 8.7 Hz, 2H), 6.40 (s, 1H), 4.24 (d, *J* = 5.7 Hz, 2H), 3.76 (s, 3H), 3.40 (d, *J* = 5.7 Hz, 2H), 2.77 (t, *J* = 7.5 Hz, 2H). <sup>13</sup>C NMR (100 MHz, DMSO-*d*<sub>6</sub>) δ: 166.07, 162.26, 161.91, 157.25, 144.27, 138.51, 138.07, 129.38, 128.98, 128.23, 127.26, 124.13, 122.96, 113.91, 110.93, 101.15, 55.78, 47.09, 41.35, 35.37. HRMS(EI) *m/z* calcd for C<sub>25</sub>H<sub>26</sub>N<sub>6</sub>O<sub>2</sub>(M<sup>+</sup>) 422.2117, found 422.2119.

4.7.7. 3-Chloro-*N*-(4-(((2,4-diaminoquinazolin-6-yl)amino)methyl)phenethyl)-4-methoxybenzamide (**15**)

Green solid, 40% yield. mp: 141–143 °C; <sup>1</sup>H NMR (400 MHz, DMSO-*d*<sub>6</sub>) δ: 7.58 (d, *J* = 8.2 Hz, 1H), 7.35 (d, *J* = 7.9 Hz, 2H), 7.27 (d, *J* = 8.2 Hz, 1H), 7.21 (d, *J* = 6.9 Hz, 3H), 7.16 (s, 2H), 7.01 (t, *J* = 7.6 Hz, 3H), 6.95 (s, 2H), 6.90 (s, 2H), 4.24 (d, *J* = 6.3 Hz, 2H), 3.92 (s, 3H), 3.17 (s, 2H), 2.67 (s, 2H). <sup>13</sup>C NMR (100 MHz, DMSO-*d*<sub>6</sub>) δ: 164.86, 162.53, 157.08, 155.92, 145.02, 138.45, 137.91, 129.16, 129.00, 128.21, 127.97, 124.28, 121.21, 112.74, 110.80, 101.36, 56.86, 46.94, 41.41, 35.22. HRMS(EI) *m/z* calcd for C<sub>25</sub>H<sub>23</sub>ClN<sub>6</sub>O<sub>2</sub>(M<sup>+</sup>) 476.1728, found 476.1726.

4.7.8. *N*-(4-(((2,4-diaminoquinazolin-6-yl)amino)methyl)phenethyl)-4-fluorobenzamide (**16**)

Green solid, 43% yield. mp: 269–271 °C; <sup>1</sup>H NMR (400 MHz, DMSO-*d*<sub>6</sub>) δ: 8.59 (s, 1H), 7.95–7.84 (m, 2H), 7.38–7.16 (m, 5H), 7.10–6.84 (m, 5H), 5.86 (s, 2H), 5.44 (s, 2H), 4.25 (d, *J* = 6.2 Hz, 2H), 3.44 (s, 2H), 2.81 (s, 2H). <sup>13</sup>C NMR (100 MHz, DMSO-*d*<sub>6</sub>) δ: 174.59, 165.53, 163.02, 162.36, 157.01, 144.44, 139.74, 138.39, 138.07, 130.24, 130.15, 128.98, 128.24, 124.20, 115.75, 115.53, 110.82, 101.24, 47.04, 41.42, 35.22. HRMS(EI) *m/z* calcd for C<sub>24</sub>H<sub>23</sub>FN<sub>6</sub>O(M<sup>+</sup>) 430.1917, found 430.1918.

4.7.9. *N*-(4-(((2,4-diaminoquinazolin-6-yl)amino)methyl)phenethyl)-3-fluorobenzamide (**17**)

Green solid, 46% yield. mp: 265–267 °C; <sup>1</sup>H NMR (400 MHz, DMSO-*d*<sub>6</sub>) δ: 8.70 (d, *J* = 5.7 Hz, 2H), 8.54 (s, 2H), 7.75–7.65 (m, 1H), 7.61 (d, *J* = 9.8 Hz, 1H), 7.52 (dd, *J* = 13.7, 8.0 Hz, 2H), 7.38 (d, *J* = 7.9 Hz, 2H), 7.34 (d, *J* = 8.0 Hz, 2H), 7.26–7.17 (m, 4H), 6.53 (t, *J* = 6.3 Hz, 1H), 4.28 (d, *J* = 5.7 Hz, 2H), 3.46 (dd, *J* = 14.1, 6.5 Hz, 2H), 2.82 (t, *J* = 7.5 Hz, 2H). <sup>13</sup>C NMR (100 MHz, DMSO-*d*<sub>6</sub>) δ: 165.22, 163.03, 161.20, 153.70, 146.42, 138.46, 137.64, 130.89, 130.78, 129.03, 128.21, 124.64, 123.75, 118.17, 118.01, 114.51, 114.29, 110.52, 101.93, 46.71, 41.43, 35.11. HRMS(EI) *m/z* calcd for C<sub>24</sub>H<sub>23</sub>FN<sub>6</sub>O(M<sup>+</sup>) 430.1917, found 430.1915.

4.7.10. *N*-(4-(((2,4-diaminoquinazolin-6-yl)amino)methyl)phenethyl)-2-fluorobenzamide (**18**)

Green solid, 40% yield. mp: 108–110 °C; <sup>1</sup>H NMR (400 MHz, DMSO-*d*<sub>6</sub>) δ: 8.41 (s, 1H), 7.53 (dt, *J* = 21.1, 6.6 Hz, 2H), 7.36 (d, *J* = 7.8 Hz, 2H), 7.31–7.17 (m, 4H), 7.02 (q, *J* = 8.9 Hz, 2H), 6.94 (d, *J* = 14.8 Hz, 3H), 5.89 (t, *J* = 5.9 Hz, 1H), 5.47 (s, 2H), 4.25 (d, *J* = 5.8 Hz, 2H), 3.52–3.43 (m, 2H), 2.80 (t, *J* = 7.4 Hz, 2H). <sup>13</sup>C NMR (100 MHz, DMSO-*d*<sub>6</sub>) δ: 164.07, 161.89, 160.77, 158.79, 158.29, 145.54, 143.31, 138.40, 138.19, 130.46, 130.43, 128.98, 128.26, 125.47, 124.92, 124.89, 123.89, 116.65, 116.43, 111.21, 100.90, 47.26, 41.34, 35.11. HRMS(EI) *m/z* calcd for C<sub>24</sub>H<sub>23</sub>FN<sub>6</sub>O(M<sup>+</sup>) 430.1917, found 430.1920.

4.7.11. 4-Chloro-*N*-(4-(((2,4-diaminoquinazolin-6-yl)amino)methyl)phenethyl)-2-fluorobenzamide (**19**)

Green solid, 44% yield. mp: 178–180 °C; <sup>1</sup>H NMR (400 MHz, DMSO-*d*<sub>6</sub>) δ: 8.70 (s, 1H), 8.44 (t, *J* = 5.6 Hz, 1H), 7.96 (d, *J* = 2.0 Hz, 2H), 7.87 (d, *J* = 8.0 Hz, 2H), 7.61–7.54 (m, 2H), 7.41 (d, *J* = 8.0 Hz, 2H), 7.37–7.20 (m, 6H), 4.20 (s, 2H), 3.52 (dd, *J* = 12.7, 6.7 Hz, 2H), 2.91 (t, *J* = 6.9 Hz, 2H). <sup>13</sup>C NMR (100 MHz, DMSO-*d*<sub>6</sub>) δ: 168.68, 163.15, 160.60, 158.84, 143.42, 143.23, 138.52, 136.38, 134.90, 134.01, 129.72, 129.37, 128.90, 127.35, 125.87, 116.30, 110.71, 47.34, 41.52, 35.05. HRMS(EI) *m/z* calcd for C<sub>24</sub>H<sub>22</sub>ClFN<sub>6</sub>O(M<sup>+</sup>) 464.1528, found 464.1530.

4.7.12. *N*-(4-(((2,4-diaminoquinazolin-6-yl)amino)methyl)phenethyl)-4-(trifluoromethyl)benzamide (**20**)

Green solid, 65% yield. mp: 167–169 °C; <sup>1</sup>H NMR (400 MHz, DMSO-*d*<sub>6</sub>) δ: 8.79 (t, *J* = 5.5 Hz, 1H), 8.44 (s, 1H), 8.10 (d, *J* = 8.0 Hz, 1H), 7.98 (d, *J* = 8.1 Hz, 2H), 7.82 (d, *J* = 8.4 Hz, 2H), 7.73 (d, *J* = 8.1 Hz, 1H), 7.36 (s, 2H), 7.32 (d, *J* = 8.0 Hz, 2H), 7.23–7.16 (m, 3H), 7.11 (dd, *J* = 14.0, 6.3 Hz, 2H), 6.44 (t, *J* = 5.9 Hz, 1H), 4.26 (d, *J* = 5.7 Hz, 2H), 3.47 (m, 2H), 2.82 (dd, *J* = 14.7, 7.1 Hz, 2H). <sup>13</sup>C NMR (100 MHz, DMSO-*d*<sub>6</sub>) δ: 172.60, 165.82, 163.11, 162.89, 158.36, 151.20, 141.23, 140.04, 138.54, 132.01, 131.56, 129.54, 127.69, 123.91, 123.60, 116.35, 111.79, 102.32, 46.64, 41.33, 35.22. HRMS(EI) *m/z* calcd for C<sub>25</sub>H<sub>23</sub>F<sub>3</sub>N<sub>6</sub>O(M<sup>+</sup>) 480.1885, found 480.1887.

4.7.13. *N*-(4-(((2,4-diaminoquinazolin-6-yl)amino)methyl)phenethyl)-4-nitrobenzamide (**21**)

Green solid, 70% yield. mp: 148–150 °C; <sup>1</sup>H NMR (400 MHz, DMSO-*d*<sub>6</sub>) δ: 8.89 (t, *J* = 5.6 Hz, 1H), 8.50 (s, 2H), 8.27 (d, *J* = 8.8 Hz, 2H), 8.00 (d, *J* = 8.7 Hz, 2H), 7.30 (d, *J* = 7.9 Hz, 4H), 7.17 (t, *J* = 11.4 Hz, 6H), 6.47 (t, *J* = 5.9 Hz, 1H), 4.24 (d, *J* = 5.7 Hz, 2H), 3.50–3.44 (m, 2H), 2.82 (dd, *J* = 17.0, 9.7 Hz, 2H). <sup>13</sup>C NMR (100 MHz, DMSO-*d*<sub>6</sub>) δ: 172.60, 164.96, 163.21, 162.30, 157.26, 149.41, 140.63, 138.34, 137.74, 129.08, 129.04, 128.19, 124.51, 124.00, 115.45, 110.59, 101.72, 46.74, 41.53, 35.02. HRMS(EI) *m/z* calcd for C<sub>24</sub>H<sub>23</sub>N<sub>7</sub>O<sub>3</sub>(M<sup>+</sup>) 457.1862, found 457.1863.

4.7.14. *N*-(4-(((2,4-diaminoquinazolin-6-yl)amino)methyl)phenethyl)isonicotinamide (**22**)

Green solid, 40% yield. mp: 270–272 °C; <sup>1</sup>H NMR (400 MHz, DMSO-*d*<sub>6</sub>) δ: 9.28 (s, 1H), 8.84 (d, *J* = 6.7 Hz, 2H), 8.69 (d, *J* = 5.6 Hz, 2H), 8.47 (s, 2H), 8.15 (d, *J* = 6.6 Hz, 1H), 7.69 (d, *J* = 4.4 Hz, 2H), 7.22 (m, 8H), 4.35 (m, 2H), 3.41 (m, 2H), 2.71 (m, 2H). <sup>13</sup>C NMR (100 MHz, DMSO-*d*<sub>6</sub>) δ: 171.50, 164.62, 163.51, 162.29, 159.06, 152.30, 142.13, 141.14, 139.24, 133.61, 131.06, 128.24, 128.09, 125.11, 124.50, 124.32, 110.59, 46.44, 41.53, 35.21. HRMS(EI) *m/z* calcd for C<sub>23</sub>H<sub>23</sub>N<sub>7</sub>O(M<sup>+</sup>) 413.1964, found 413.1965.

4.7.15. *N*-(4-(((2,4-diaminoquinazolin-6-yl)amino)methyl)phenethyl)furan-2-carboxamide (**23**)

Green solid, 41% yield. mp: 156–158 °C; <sup>1</sup>H NMR (400 MHz, DMSO-*d*<sub>6</sub>) δ: 8.41 (t, *J* = 5.4 Hz, 1H), 8.05 (s, 2H), 7.78 (s, 1H), 7.30 (d, *J* = 7.8 Hz, 2H), 7.25–6.97 (m, 6H), 6.77 (s, 2H), 6.57 (s, 1H), 6.29 (s, 1H), 4.23 (d, *J* = 5.6 Hz, 2H), 3.39 (s, 2H), 2.78–2.70 (m, 2H). <sup>13</sup>C NMR (100 MHz, DMSO-*d*<sub>6</sub>) δ: 162.99, 158.14, 153.83, 148.43, 146.34, 145.33, 138.40, 137.64, 131.26, 128.99, 128.21, 124.61, 118.27, 113.64, 112.25, 110.54, 101.87, 46.73, 45.85, 35.25. HRMS(EI) *m/z* calcd for C<sub>22</sub>H<sub>22</sub>N<sub>6</sub>O<sub>2</sub>(M<sup>+</sup>) 402.1804, found 402.1803.

4.7.16. *N*-(4-(((2,4-diaminoquinazolin-6-yl)amino)methyl)phenethyl)thiophene-2-carboxamide (**24**)

Green solid, 46% yield. mp: 170–172 °C; <sup>1</sup>H NMR (400 MHz, DMSO-*d*<sub>6</sub>) δ: 8.58 (s, 1H), 8.25 (s, 2H), 7.69 (d, *J* = 3.8

Hz, 2H), 7.30 (d,  $J = 7.6$  Hz, 2H), 7.25–6.90 (m, 8H), 6.37 (s, 1H), 4.24 (d,  $J = 5.0$  Hz, 2H), 3.38 (s, 2H), 2.83–2.68 (m, 2H).  $^{13}\text{C}$  NMR (100 MHz, DMSO- $d_6$ )  $\delta$ : 162.88, 161.50, 154.38, 146.02, 140.60, 138.42, 137.74, 132.75, 131.02, 129.01, 128.38, 128.22, 124.54, 119.00, 110.62, 101.81, 46.79, 45.86, 35.29. HRMS(EI)  $m/z$  calcd for  $\text{C}_{22}\text{H}_{22}\text{N}_6\text{O}(\text{M}^+)$  418.1576, found 418.1579.

4.7.17. *N*-(4-(((2,4-diaminoquinazolin-6-yl)amino)methyl)phenethyl)-2-naphthamide (25)

Green solid, 57% yield. mp: 235–237 °C;  $^1\text{H}$  NMR (400 MHz, DMSO- $d_6$ )  $\delta$ : 8.75 (s, 1H), 8.42 (s, 1H), 7.98 (d,  $J = 8.9$  Hz, 3H), 7.91 (d,  $J = 8.7$  Hz, 1H), 7.60 (s, 2H), 7.37 (d,  $J = 7.6$  Hz, 2H), 7.23 (d,  $J = 7.7$  Hz, 2H), 7.01 (t,  $J = 7.1$  Hz, 2H), 6.93 (d,  $J = 21.9$  Hz, 3H), 5.87 (s, 1H), 5.44 (s, 2H), 4.26 (s, 2H), 3.51 (s, 2H), 2.87 (s, 2H).  $^{13}\text{C}$  NMR (100 MHz, DMSO- $d_6$ )  $\delta$ : 162.76, 161.85, 158.83, 146.45, 143.26, 138.37, 134.53, 132.43, 131.52, 129.28, 128.98, 128.08, 127.78, 127.19, 124.60, 123.87, 119.52, 111.22, 100.87, 46.50, 45.65, 35.30. HRMS(EI)  $m/z$  calcd for  $\text{C}_{28}\text{H}_{26}\text{N}_6\text{O}(\text{M}^+)$  462.2168, found 462.2166.

4.7.18. *N*-(4-(((2,4-diaminoquinazolin-6-yl)amino)methyl)phenethyl)-2-phenylacetamide (26)

Green solid, 51% yield. mp: 220–223 °C;  $^1\text{H}$  NMR (400 MHz, DMSO- $d_6$ )  $\delta$ : 8.67 (s, 1H), 8.54 (s, 1H), 8.07 (s, 1H), 7.76–7.63 (m, 4H), 7.39 (s, 2H), 7.27–7.15 (m, 6H), 7.08 (d,  $J = 7.8$  Hz, 2H), 6.52 (t,  $J = 5.7$  Hz, 1H), 4.26 (d,  $J = 5.4$  Hz, 2H), 4.14 (p,  $J = 11.1$  Hz, 4H), 2.63 (t,  $J = 7.2$  Hz, 2H).  $^{13}\text{C}$  NMR (100 MHz, DMSO- $d_6$ )  $\delta$ : 173.07, 162.94, 154.12, 146.17, 141.70, 138.43, 137.61, 129.00, 128.56, 128.07, 126.87, 124.55, 118.53, 110.58, 101.96, 51.66, 46.69, 35.14, 33.12. HRMS(EI)  $m/z$  calcd for  $\text{C}_{25}\text{H}_{26}\text{N}_6\text{O}(\text{M}^+)$  426.2168, found 426.2168.

4.7.19. *N*-(4-(((2,4-diaminoquinazolin-6-yl)amino)methyl)phenethyl)-3-phenylpropanamide (27)

Green solid, 56% yield. mp: 218–221 °C;  $^1\text{H}$  NMR (400 MHz, DMSO- $d_6$ )  $\delta$ : 7.82 (s, 1H), 7.28 (dd,  $J = 20.3, 7.7$  Hz, 5H), 7.15 (d,  $J = 7.6$  Hz, 3H), 7.09–6.86 (m, 6H), 5.85 (s, 1H), 5.43 (s, 2H), 4.23 (d,  $J = 5.3$  Hz, 2H), 3.14 (d,  $J = 6.4$  Hz, 2H), 2.98 (s, 2H), 2.53 (s, 2H), 2.37–2.22 (m, 2H).  $^{13}\text{C}$  NMR (100 MHz, DMSO- $d_6$ )  $\delta$ : 171.17, 161.86, 158.83, 145.69, 145.24, 143.25, 138.34, 138.28, 128.86, 128.64, 128.19, 127.88, 126.45, 125.56, 123.87, 111.22, 100.89, 47.20, 43.34, 42.23, 35.57, 35.31. HRMS(EI)  $m/z$  calcd for  $\text{C}_{26}\text{H}_{28}\text{N}_6\text{O}(\text{M}^+)$  440.2325, found 440.2323.

4.7.20. *N*-(4-(((2,4-diaminoquinazolin-6-yl)amino)methyl)phenethyl)cyclohexanecarboxamide (28)

Green solid, 62% yield. mp: 118–120 °C;  $^1\text{H}$  NMR (400 MHz, DMSO- $d_6$ )  $\delta$ : 11.83 (s, 1H), 8.62 (s, 1H), 8.49 (s, 1H), 7.70 (s, 1H), 7.35 (s, 2H), 7.27 (d,  $J = 8.0$  Hz, 2H), 7.19 (s, 2H), 7.12 (d,  $J = 8.2$  Hz, 2H), 6.49 (s, 1H), 4.24 (d,  $J = 5.8$  Hz, 2H), 3.22–3.12 (m, 2H), 2.68–2.59 (m, 2H), 1.99 (s, 2H), 1.59 (d,  $J = 19.2$  Hz, 5H), 1.32–1.01 (m, 4H).  $^{13}\text{C}$  NMR (100 MHz, DMSO- $d_6$ )  $\delta$ : 172.01, 161.20, 159.52, 142.20, 138.41, 137.52, 129.89, 128.67, 128.10, 127.01, 125.50, 124.67, 110.67, 100.65, 47.01, 36.75, 35.21, 33.55, 30.02, 25.50, 25.03. HRMS(EI)  $m/z$  calcd for  $\text{C}_{24}\text{H}_{30}\text{N}_6\text{O}(\text{M}^+)$  418.2481, found 418.2482.

4.7.21. 4-(*Tert*-butyl)-*N*-(4-(((2,4-diaminoquinazolin-6-yl)amino)methyl)phenethyl)cyclohexane-1-carboxamide (29)

Green solid, 60% yield. mp: 99–102 °C;  $^1\text{H}$  NMR (400 MHz, DMSO- $d_6$ )  $\delta$ : 7.75 (s, 1H), 7.70–7.63 (m, 1H), 7.33 (d,  $J = 7.7$  Hz, 2H), 7.15 (s, 2H), 7.07–6.98 (m, 2H), 6.95 (s, 1H), 6.89 (s, 1H), 5.85 (s, 1H), 5.43 (s, 2H), 4.24 (s, 2H), 3.26–3.15 (m,

3H), 2.67 (s, 3H), 2.33 (s, 2H), 1.99 (s, 3H), 1.74 (s, 3H), 0.80 (m, 9H).  $^{13}\text{C}$  NMR (100 MHz, DMSO- $d_6$ )  $\delta$ : 171.61, 162.42, 160.51, 143.00, 139.11, 136.02, 130.09, 127.97, 127.50, 127.06, 126.40, 125.47, 111.77, 101.65, 46.61, 36.65, 35.41, 33.05, 32.28, 31.02, 28.65, 25.90, 25.33. HRMS(EI)  $m/z$  calcd for  $\text{C}_{28}\text{H}_{38}\text{N}_6\text{O}(\text{M}^+)$  474.3107, found 474.3105.

4.8. Enzyme inhibition assays against FP-2 and PfDHFR

FP-2 (30 nM) was incubated with different concentrations of tested compounds for 30 min at room temperature in the solution of 100 mM sodium acetate and 10 mM DTT (pH 5.5). Compound solutions were prepared from stock in DMSO (maximum concentration of DMSO in the assay was 1%). After 30 min incubation, the substrate Z-Leu-Arg-AMC (benzoxycarbonyl-Leu-Arg-7-amino-4-methylcoumarin, Bachem AG) in the same buffer was added to a final concentration of 25  $\mu\text{M}$ . The increase in fluorescence (excitation at 355 nm and emission at 460 nm) was monitored for 30 min at room temperature with an automated microtiter plate spectrofluorimeter (Molecular Devices, Flex station). *P. falciparum* DHFR inhibitory activity assays were carried out in 96-well plates in a total assay volume of 200  $\mu\text{L}$ . The spectrophotometrically assay was based on measuring the oxidation of NADPH to NADP $^+$  at 340 nm. The purified DHFR was incubated for 15 min on ice in assay buffer (100  $\mu\text{M}$  NADPH, 50 mM TES, pH 7.0, 1 mM EDTA, pH 8.0, 75 mM 2-mercaptoethanol, 1 mg/mL bovine serum albumin), with various concentrations of compounds to be tested. After 15 min incubation, the reaction was initiated with 100  $\mu\text{M}$  DHF. Half-maximal inhibitory concentration (IC $_{50}$ ) values were calculated from plots of percentage inhibition of FP-2 and PfDHFR activities against various compounds concentration using the GraphPad Prism software with three independent experiments.

4.9. In vitro inhibition assays against *P. falciparum*

*P. falciparum* clones 3D7, Dd2, Fab9 and GB4 were cultured in human O $^+$  erythrocytes according to standard procedures<sup>[18]</sup>. To prepare the > 80% ring stage parasites, the asynchronous cultures of parasites were pretreated with 5% sorbital. *Plasmodium falciparum* strains mentioned in the text at the mid-ring stage (6–10 h postinvasion) were used to test antimalarial effects in 96-well plates. Parasites were incubated in a 96-well plate with 10, 13, 16, 21, 24, 26, Artemisinin, or pyrimethamine at equal ratio containing 1% parasitemia, 2% hematocrit for total 200  $\mu\text{L}$ . For 3D7 the compounds were from the maximum concentration of 200 nM, for Dd2 were from 10  $\mu\text{M}$  as the maximum concentration. The parasites were allowed to grow for 72 h at 37 °C with 5% CO $_2$ , 5% O $_2$ , 90% N $_2$ . After 72 h, add 100  $\mu\text{L}$  of lysis buffer (0.12 mg/mL Saponin, 0.12% Triton X-100 30 mM Tris-Cl, 7.5 mM EDTA) consisting 5X SYBR Green I (Invitrogen; supplied in 10000  $\times$  concentration) to each well of the plate, the plates were then incubated for 2 h in dark prior to reading the fluorescence signal on instrument at 485 nm excitation and 535 nm emission.

4.10. In vivo inhibition assays

Three BALB/c mice per treatment group were infected with  $5 \times 10^6$  *P. berghei* ANKA strain parasites. Mice were treated with 20 mg/kg orally of test compounds or control (Art and pyrimethamine) each day for 4 days' treatments after 24 hours. Parasitemia was quantified by Giemsa-stained blood sample smear every day for a total 10 days' observation.

4.11. Molecular docking and binding power prediction

The crystal structures of falcipain-2 (FP-2) binding with cystatin and *P. falciparum* dihydrofolate reductase (PfDHFR) binding with WRA from *Plasmodium falciparum* were retrieved from the Protein Data Bank (PDB entry: 2OUL and 1J3I, respectively). All crystallographic water molecules were removed from the coordinate set. Hydrogen atoms and charges were added using the Protein Preparation Wizard in Maestro v9.0, and a restrained partial minimization was terminated when the root-mean-square deviation (rmsd) reached a maximum value of 0.3 Å in order to relieve steric clashes. Glide v5.5 (Schrodinger, Inc.) was used for molecular docking. The grid-enclosing boxes were centered on the bound ligands and defined so as to enclose residues located within 14 Å from the ligands in FP-2 and PfDHFR, respectively. A scaling factor of 1.0 was set to van der Waals (VDW) radii of those receptor atoms with the partial atomic charge less than 0.25. The initial 3D structures of 31, compounds A-C, analogues 13 and 24 were generated with the help of LigPrep v2.3 (Schrodinger, Inc.). In the docking process, standard-precision (SP) and extra-precision (XP) docking modes were respectively adopted to generate the minimized poses, the Glide scoring function (G-Score) was referred to select at most 10 poses for 13 and 24 upon visualized observation.

### Acknowledgments

Financial support for this research provided by the National Natural Science Foundation of China (Grants 21372001 and 21672064), the “Shu Guang” project supported by the Shanghai Municipal Education Commission and Shanghai Education Development Foundation (Grant 14SG28), and the Fundamental Research Funds for the Central Universities are gratefully acknowledged.

### References and notes

- Persidis, A. *Malaria. Nat. Biotechnol.* **2000**, *18*, 111–112.
- Conroy, T.; Guo, J. T.; Elias, N.; Cergol, K. M.; Gut, J.; Legac, J.; Khatoon, L.; Liu, Y.; McGowan, S.; Rosenthal, P. J.; Hunt, N. H.; Payne, R. J. Synthesis of gallinamide analogues as potent falcipain inhibitors and antimalarials. *J. Med. Chem.* **2014**, *57*, 10557–10563.
- Hotez, P. J.; Pecoul, B. “Manifesto” for advancing the control and elimination of neglected tropical diseases. *PLoS Neglected Trop. Dis.* **2010**, *4*, e718.
- World Malaria Report 2016; World Health Organization: Geneva. <http://www.who.int/malaria/publications/world-malaria-report-2016/en/>, **2016**.
- Zhang, Y. K.; Platter, J. J.; Easom, E. E.; Jacobs, R. T.; Guo, D. H.; Freund, Y. R.; Bery, P.; Ciaravino, V.; Erve, J. C. L.; Rosenthal, P. J.; Campo, B.; Gamo, F. J.; Sanz, L. M.; Cao, J. X. Benzoxaborole antimalarial agents. Part 5. Lead optimization of novel amide pyrazinyloxy benzoxaboroles and identification of a preclinical candidate. *J. Med. Chem.* **2017**, *60*, 5889–5908.
- White, N. J.; Pukrittayakamee, S.; Hien, T. T.; Faiz, M. A.; Mokuolu, O. A.; Dondorp, A. M. *Malaria. Lancet.* **2014**, *383*, 723–735.
- Singh, K.; Okombo, J.; Brunshwig, C.; Ndubi, F.; Barnard, L.; Wilkinson, C.; Njogu, P. M.; Njoroge, M.; Laing, L.; Machado, M.; Prudêncio, M.; Reader, J.; Botha, M.; Nondaba, S.; Birkholtz, L. M.; Lauterbach, S.; Churchyard, A.; Coetzer, T. L.; Burrows, J. N.; Yeates, C.; Denti, P.; Wiesner, L.; Egan, T. J.; Wittlin, S.; Chibale, K. Antimalarial pyrido[1,2-*a*]benzimidazoles: Lead optimization, parasite life cycle stage profile, mechanistic evaluation, killing kinetics, and in vivo oral efficacy in a mouse model. *J. Med. Chem.* **2017**, *60*, 1432–1448.
- de Koning-Ward, T. F.; Dixon, M. W. A.; Tilley, L.; Gilson, P. R. *Plasmodium* species: Master renovators of their host cells. *Nat. Rev. Microbiol.* **2016**, *14*, 494–507.
- Mendis, K.; Sina, B. J.; Marchesini, P.; Carter, R. The neglected burden of *Plasmodium vivax* malaria. *Am. J. Trop. Med. Hyg.* **2001**, *64*, 97–106.
- Autino, B.; Corbett, Y.; Castelli, F.; Taramelli, D. Pathogenesis of malaria in tissues and blood. *Mediterr. J. Hematol. Infect. Dis.* **2012**, *4*, e2012061.
- Gazzinelli, R. T.; Kalantari, P.; Fitzgerald, K. A.; Golenbock, D. T. Innate sensing of malaria parasites. *Nat. Rev. Immunol.* **2014**, *14*, 744–757.
- Pieroni, M.; Azzali, E.; Basilico, N.; Parapini, S.; Zolkiewski, M.; Beato, C.; Annunziato, G.; Bruno, A.; Vacondio, F.; Costantino, G. Accepting the invitation to open innovation in malaria drug discovery: Synthesis, biological evaluation, and investigation on the structure-activity relationships of benzo[*b*]thiophene-2-carboxamides as antimalarial agents. *J. Med. Chem.* **2017**, *60*, 1959–1970.
- Musset, L.; Bouchaud, O.; Matheron, S.; Massias, L.; Le Bras, J. Clinical atovaquone-proguanil resistance of *Plasmodium falciparum* associated with cytochrome *b* codon 268 mutations. *Microbes Infect.* **2006**, *8*, 2599–2604.
- Dondorp, A. M.; Nosten, F.; Yi, P.; Das, D.; Phyto, A. P.; Tarning, J.; Lwin, K. M.; Ariey, F.; Hanpithakpong, W.; Lee, S. J.; Ringwald, P.; Silamut, K.; Imwong, M.; Chotivanich, K.; Lim, P.; Herdman, T.; An, S. S.; Yeung, S.; Singhasivanon, P.; Day, N. P.; Lindegardh, N.; Socheat, D.; White, N. J. Artemisinin resistance in *Plasmodium falciparum* malaria. *N. Engl. J. Med.* **2009**, *361*, 455–467.
- Dondorp, A. M.; Yeung, S.; White, L.; Nguon, C.; Day, N. P.; Socheat, D.; von Seidlein, L. Artemisinin resistance: current status and scenarios for containment. *Nat. Rev. Microbiol.* **2010**, *8*, 272–280.
- Ariey, F.; Witkowski, B.; Amaratunga, C.; Beghain, J.; Langlois, A. C.; Khim, N.; Kim, S.; Duru, V.; Bouchier, C.; Ma, L.; Lim, P.; Leang, R.; Duong, S.; Sreng, S.; Suon, S.; Chhior, C. M.; Bout, D. M.; Menard, S.; Rogers, W. O.; Genton, B.; Fandeur, T.; Miotto, O.; Ringwald, P.; Le Bras, J.; Berry, A.; Barale, J. C.; Fairhurst, R. M.; Benoit-Vical, F.; Mercereau-Puijalon, O.; Menard, D. A molecular marker of artemisinin-resistant *Plasmodium falciparum* malaria. *Nature* **2014**, *505*, 50–55.
- St. Laurent, B.; Miller, B.; Burton, T. A.; Amaratunga, C.; Men, S.; Sovannaroeth, S.; Fay, M. P.; Miotto, O.; Gwadz, R. W.; Anderson, J. M.; Fairhurst, R. M. Artemisinin-resistant *Plasmodium falciparum* clinical isolates can infect diverse mosquito vectors of Southeast Asia and Africa. *Nat. Commun.* **2015**, *6*, 8614.
- Yang, Y. Q.; Yu, Y.; Li, X. L.; Li, J.; Wu, Y.; Yu, J.; Ge, J. P.; Huang, Z. H.; Jiang, L. B.; Rao, Y.; Yang, M. J. Target elucidation by cocrystal structures of NADH-ubiquinone oxidoreductase of *Plasmodium falciparum* (PfNDH2) with small molecule to eliminate drug-resistant malaria. *J. Med. Chem.* **2017**, *60*, 1994–2005.
- Andrews, K. T.; Fisher, G.; Skinner-Adams, T. S. Drug repurposing and human parasitic protozoan diseases. *Int. J. Parasitol.: Drugs Drug Resist.* **2014**, *4*, 95–111.
- Gilson, P. R.; Tan, C.; Jarman, K. E.; Lowes, K. N.; Curtis, J. M.; Nguyen, W.; Di Rago, A. E.; Bullen, H. E.; Prinz, B.; Duffy, S.; Baell, J. B.; Hutton, C. A.; Subroux, H. J.; Crabb, B. S.; Avery, V. M.; Cowman, A. F.; Sleebs, B. E. Optimization of 2-anilino-4-amino substituted quinazolines into potent antimalarial agents with oral in vivo activity. *J. Med. Chem.* **2017**, *60*, 1171–1188.
- Flannery, E. L.; Wang, T.; Akbari, A.; Corey, V. C.; Gunawan, F.; Bright, A. T.; Abraham, M.; Sanchez, J. F.; Santolalla, M. L.; Baldeviano, G. C.; Edgel, K. A.; Rosales, L. A.; Lescano, A. G.; Bafna, V.; Vinetz, J. M.; Winzeler, E. A. Next-generation sequencing of *Plasmodium vivax* patient samples shows evidence of direct evolution in drug-resistance genes. *ACS Infect. Dis.* **2015**, *1*, 367–379.
- Sourabh M.; Vandana T.; Angelica M. B.; Sumit R.; Mohd A.; Lianhu W.; Jane Y.; Sai K. C.; Radhakrishnan M.; Pawan M. A novel class of Plasmodial ClpP protease inhibitors as potential antimalarial agents. *Bioorg. Med. Chem.* **2017**, <https://doi.org/10.1016/j.bmc.2017.08.049>.
- Petr Š.; Dianne T. K.; Marina C.; Martin D.; Zlatko J.; Lieve N.; Michael D. E.; Luke W. G.; Dana H. Synthesis and evaluation of symmetric acyclic nucleoside bisphosphonates as inhibitors of the *Plasmodium falciparum*, *Plasmodium vivax* and human 6-oxopurine phosphoribosyltransferases and the antimalarial activity of their prodrugs. *Bioorg. Med. Chem.* **2017**, *25*, 4008–4030.
- Sampark S. T.; Parth T.; Hiren D.; Arabinda R. 1,2,4-Triazole and 1,3,4-oxadiazole analogues: Synthesis, MO studies, *in silico* molecular docking studies, antimalarial as DHFR inhibitor and antimicrobial activities. *Bioorg. Med. Chem.* **2017**, *25*, 4064–4075.
- Marvin J. M.; Elizabeth J. A.; Sarah A. M.; Thomas M. K.; Megh S.; Jing X.; Wentian Z.; Limei Q.; Wanwan X.; Siting Z.; Li Q.; Christopher S. E.; Jonathan O.; Mary A. C.; Stacy D. A.; Michael J. P.; David W. G.; Peter G. R.; Xiaoping C. Evaluation of spiroperidine hydantoinis as a novel class of antimalarial agents. *Bioorg. Med. Chem.* **2015**, *23*, 5144–5150.
- Miller, L. H.; Baruch, D. I.; Marsh, K.; Doumbo, O. K. The pathogenic basis of malaria. *Nature*. **2002**, *415*, 673–679.
- Singh, A.; Rosenthal, P. J. Selection of cysteine protease inhibitor-resistant malaria parasites is accompanied by amplification of falcipain

- genes and alteration in inhibitor transport. *J. Biol. Chem.* **2004**, *279*, 35236–35241.
28. Arafet, K.; Ferrer, S.; Martí, S.; Moliner, V. Quantum mechanics/molecular mechanics studies of the mechanism of falcipain-2 inhibition by the epoxysuccinate E64. *Biochemistry.* **2014**, *53*, 3336–3346.
  29. Stolze, S. C.; Deu, E.; Kaschani, F.; Li, N.; Florea, B. I.; Richau, K. H.; Colby, T.; van der Hooft, R. A. L.; Overkleeft, H. S.; Bogyo, M.; Kaiser, M. The antimalarial natural product symplostatin 4 is a nanomolar inhibitor of the food vacuole falcipains. *Chem. Biol.* **2012**, *19*, 1546–1555.
  30. Musyoka, T. M.; Kanzi, A. M.; Lobb, K. A.; Bishop, Ö. T. Analysis of non-peptidic compounds as potential malarial inhibitors against *Plasmodium* cysteine proteases via integrated virtual screening workflow. *J. Biomol. Struct. Dyn.* **2016**, *35*, 2084–2101.
  31. Sijwali, P. S.; Rosenthal, P. J. Gene disruption confirms a critical role for the cysteine protease falcipain-2 in hemoglobin hydrolysis by *Plasmodium falciparum*. *Proc. Natl. Acad. Sci. U. S. A.* **2004**, *101*, 4384–4389.
  32. Sijwali, P. S.; Koo, J.; Singh, N.; Rosenthal, P. J. Gene disruptions demonstrate independent roles for the four falcipain cysteine proteases of *Plasmodium falciparum*. *Mol. Biochem. Parasitol.* **2006**, *150*, 96–106.
  33. Verissimo, E.; Berry, N.; Gibbons, P.; Cristiano, M. L. S.; Rosenthal, P. J.; Gut, J.; Ward, S. A.; O'Neill, P. M. Design and synthesis of novel 2-pyridone peptidomimetic falcipain 2/3 inhibitors. *Bioorg. Med. Chem. Lett.* **2008**, *18*, 4210–4214.
  34. Kerr, I. D.; Lee, J. H.; Farady, C. J.; Marion, R.; Rickert, M.; Sajid, M.; Pandey, K. C.; Caffrey, C. R.; Legac, J.; Hansell, E.; McKerrow, J. H.; Craik, C. S.; Rosenthal, P. J.; Brinen, L. S. Vinyl sulfones as antiparasitic agents and a structural basis for drug design. *J. Biol. Chem.* **2009**, *284*, 25697–25703.
  35. Coteron, J. M.; Catterick, D.; Castro, J.; Chaparro, M. A. J.; Díaz, B.; Fernandez, E.; Ferrer, S.; Gamo, F. J.; Gordo, M.; Gut, J.; de las Heras, L.; Legac, J.; Marco, M.; Miguel, J.; Muñoz, V.; Porras, E.; de la Rosa, J. C.; Ruiz, J. R.; Sandoval, E.; Ventosa, P.; Rosenthal, P. J.; Fiandor, J. M. Falcipain inhibitors: optimization studies of the 2-pyrimidinocarbonitrile lead series. *J. Med. Chem.* **2010**, *53*, 6129–6152.
  36. Breuning, A.; Degel, B.; Schulz, F.; Büchold, C.; Stempka, M.; Machon, U.; Heppner, S.; Gelhaus, C.; Leippe, M.; Leyh, M.; Kisker, C.; Rath, J.; Stich, A.; Gut, J.; Rosenthal, P. J.; Schmuck, C.; Schirmeister, T. Michael acceptor based antiplasmodial and antitypanosomal cysteine protease inhibitors with unusual amino acids. *J. Med. Chem.* **2010**, *53*, 1951–1963.
  37. Shah, F.; Mukherjee, P.; Gut, J.; Legac, J.; Rosenthal, P. J.; Tekwani, B. L.; Avery, M. A. Identification of novel malarial cysteine protease inhibitors using structure-based virtual screening of a focused cysteine protease inhibitor library. *J. Chem. Inf. Model.* **2011**, *51*, 852–864.
  38. Shah, F.; Gut, J.; Legac, J.; Shivakumar, D.; Sherman, W.; Rosenthal, P. J.; Avery, M. A. Computer-aided drug design of falcipain inhibitors: virtual screening, structure-activity relationships, hydration site thermodynamics, and reactivity analysis. *J. Chem. Inf. Model.* **2012**, *52*, 696–710.
  39. Ettari, R.; Bova, F.; Zappala, M.; Grasso, S.; Micale, N. Falcipain-2 inhibitors. *Med. Res. Rev.* **2010**, *30*, 136–167.
  40. Conroy, T.; Guo, J. T.; Elias, N.; Cergol, K. M.; Gut, J.; Legac, J.; Khatoon, L.; Liu, Y.; McGowan, S.; Rosenthal, P. J.; Hunt, N. H.; Payne, R. J. Synthesis of gallinamide A analogues as potent falcipain inhibitors and antimalarials. *J. Med. Chem.* **2014**, *57*, 10557–10563.
  41. Marco, M.; Miguel Coteron, J. Falcipain inhibition as a promising antimalarial target. *Curr. Top. Med. Chem.* **2012**, *12*, 408–444.
  42. Sai K. C.; Mohammad K.; Srividhya S.; Lianhu W.; Sourabh M.; Radhakrishnan M.; Pawan M.; Asif M. Identification of novel class of falcipain-2 inhibitors as potential antimalarial agents. *Bioorg. Med. Chem.* **2015**, *23*, 2221–2240.
  43. Anil K. S.; Vinoth R.; Akansha P.; Prahlad C. G.; Neelu S.; Latha N.; Sandeep G.; Kailash C. P.; Brajendra K. S.; Brijesh R. Design, synthesis and biological evaluation of functionalized phthalimides: A new class of antimalarials and inhibitors of falcipain-2, a major hemoglobinase of malaria parasite. *Bioorg. Med. Chem.* **2015**, *23*, 1817–1827.
  44. Gresty, K. J.; Gray, K. A.; Bobogare, A.; Wini, L.; Taleo, G.; Hii, J.; Qin, C.; Waters, N. C. Genetic mutations in *Plasmodium falciparum* and *Plasmodium vivax* dihydrofolate reductase (DHFR) and dihydropteroate synthase (DHPS) in vanuatu and solomon islands prior to the introduction of artemisinin combination therapy. *Malar. J.* **2014**, *13*, 402–408.
  45. Metzger, V. T.; Eun, C.; Kekenus-Huskey, P. M.; Huber, G.; McCammon, J. A. Electrostatic channeling in *P. falciparum* DHFR-TS: brownian dynamics and smoluchowski modeling. *Biophys. J.* **2014**, *107*, 2394–2402.
  46. Barnett, D. S.; Guy, R. K. Antimalarials in development in 2014. *Chem. Rev.* **2014**, *114*, 11221–11241.
  47. Lamb, K. M.; G-Dayananandan, N.; Wright, D. L.; Anderson, A. C. Elucidating features that drive the design of selective antifolates using crystal structures of human dihydrofolate reductase. *Biochemistry.* **2013**, *52*, 7318–7326.
  48. Huang, H.; Lu, W. Q.; Li, X.; Cong, X. L.; Ma, H. M.; Liu, X. F.; Zhang, Y.; Che, P.; Ma, R. Q.; Li, H. L.; Shen, X.; Jiang, H. L.; Huang, J.; Zhu, J. Design and synthesis of small molecular dual inhibitor of falcipain-2 and dihydrofolate reductase as antimalarial agent. *Bioorg. Med. Chem. Lett.* **2012**, *22*, 958–962.
  49. Kiara, S. M.; Okombo, J.; Masseno, V.; Mwai, L.; Ochola, I.; Borrmann, S.; Nzila, A. *In vitro* activity of antifolate and polymorphism in dihydrofolate reductase of *Plasmodium falciparum* isolates from the Kenyan coast: emergence of parasites with Ile-164-Leu mutation. *Antimicrob. Agents. Chemother.* **2009**, *53*, 3793–3798.
  50. Nzila, A.; Rottmann, M.; Chitnumsub, P.; Kiara, S. M.; Kamchonwongpaisan, S.; Maneeruttanarungroj, C.; Taweechai, S.; Yeung, B. K. S.; Goh, A.; Lakshminarayana, S. B.; Zou, B.; Wong, J.; Ma, N. L.; Weaver, M.; Keller, T. H.; Dartois, V.; Wittlin, S.; Brun, R.; Yuthavong, Y.; Diagana, T. T. Preclinical evaluation of the antifolate QN254, 5-chloro-*N*'6'-(2,5-dimethoxy-benzyl)-*au*-nazoline-2,4,6-triamine, as an antimalarial drug candidate. *Antimicrob. Agents. Chemother.* **2010**, *54*, 2603–2610.
  51. Yuthavong, Y.; Tarnchompoo, B.; Vilaivan, T.; Chitnumsub, P.; Kamchonwongpaisan, P.; Charman, S. A.; McLennan, D. N.; White, K. L.; Vivas, L.; Bongard, E.; Thongphanchang, C.; Taweechai, S.; Vanichtanankul, J.; Rattanajak, R.; Arwon, U.; Fantauzzi, P.; Yuvanijama, J.; Charman, W. N.; Matthews, D.; Malarial dihydrofolate reductase as a paradigm for drug development against a resistance-compromised target. *PNAS.* **2012**, *109*, 16823–16828.
  52. Yuthavong, Y.; Vilaivan, T.; Chareonsethakul, N.; Kamchonwongpaisan, S.; Sirawaraporn, W.; Quarrell, R.; Lowe, G. Development of a lead inhibitor for the A16V+S108T mutant of dihydrofolate reductase from the cycloguanil-resistant strain (T9/94) of *Plasmodium falciparum*. *J. Med. Chem.* **2000**, *43*, 2738–2744.
  53. Malmquist, N. A.; Moss, T. A.; Mecheri, S.; Scherf, A.; Fuchter, M. J. Small-molecule histone methyltransferase inhibitors display rapid antimalarial activity against all blood stage forms in *Plasmodium falciparum*. *Proc. Natl. Acad. Sci. U. S. A.* **2012**, *109*, 16708–16713.

### Supplementary Material

HPLC reports for analogues 9-29. This material is available free of charge via the Internet at <http://dx.doi.org>.